The JapanFlux2024 dataset for eddy covariance observations covering Japan and East Asia from 1990 to 2023

Masahito Ueyama[1], Yuta Takao[1], Hiromi Yazawa[2], Makiko Tanaka[2], Hironori Yabuki[3], Tomo'omi Kumagai[4], Hiroki Iwata[5], Md. Abdul Awal[6], Mingyuan Du[7], Yoshinobu Harazono[8], Yoshiaki Hata[4], Takashi Hirano[9], Tsutom Hiura[4], Reiko Ide[10], Sachinobu Ishida[11], Mamoru Ishikawa[12], Kenzo Kitamura[13], Yuji Kominami[14], Shujiro Komiya[15], Ayumi Kotani[16], Yuta Inoue[14], Takashi Machimura[17], Kazuho Matsumoto[18], Yojiro Matsuura[14], Yasuko Mizoguchi[19], Shohei Murayama[20], Hirohiko Nagano[21], Taro Nakai[22], Tatsuro Nakaji[23], Ko Nakaya[24], Shinjiro Ohkubo[25], Takeshi Ohta[26,☆], Keisuke Ono[27], Taku M. Saitoh[28], Ayaka Sakabe[29], Takanori Shimizu[14], Seiji Shimoda[30], Michiaki Sugita[31], Kentaro Takagi[32], Yoshiyuki Takahashi[10], Naoya Takamura[4], Satoru Takanashi[19], Takahiro Takimoto[27], Yukio Yasuda[14], Qinxue Wang[10], Jun Asanuma[33], Hideo Hasegawa[21], Tetsuya Hiyama[34], Yoshihiro Iijima[35], Shigeyuki Ishidoya[20], Masayuki Itoh[36], Tomomichi Kato[9], Hiroaki Kondo[20], Yoshiko Kosugi[29], Tomonori Kume[37], Takahisa Maeda[20], Shoji Matsuura[27], Trofim Maximov[38], Takafumi Miyama[14], Ryo Moriwaki[39], Hiroyuki Muraoka[4], Roman Petrov[38], Jun Suzuki[40], Shingo Taniguchi[41], and Kazuhito Ichii[2]

[1]Graduate School of Agriculture, Osaka Metropolitan University, Sakai 599-8531, Japan
[2]Center for Environmental Remote Sensing (CEReS), Chiba University, Chiba 263-8522, Japan
[3]National Institute of Polar Research (NIPR), Tokyo 190-8518, Japan
[4]Graduate School of Agricultural and Life Sciences, The University of Tokyo, Tokyo 113-8657, Japan
[5]Department of Environmental Science, Faculty of Science, Shinshu University, Matsumoto 390-8621, Japan
[6]Department of Crop Botany, Bangladesh Agricultural University, Mymensingh 2202, Bangladesh
[7]Xinjiang Institute of Ecology and Geography, Chinese Academy of Sciences, Xinjiang 830011, China
[8]International Arctic Research Center, University of Alaska Fairbanks, Fairbanks, AK 99775, USA
[9]Research Faculty of Agriculture, Hokkaido University, Sapporo 060-8589, Japan
[10]National Institute for Environmental Studies, Tsukuba 305-8506, Japan
[11]Graduate School of Science and Technology, Hirosaki University, Hirosaki 036-8561, Japan
[12]Faculty of Earth Environmental Science, Hokkaido University, Sapporo 060-0810, Japan
[13]Kyushu Research Center, Forestry and Forest Products Research Institute, Kumamoto 860-0862, Japan
[14]Forestry and Forest Products Research Institute, Tsukuba 305-8687, Japan
[15]Department of Biogeochemical Processes, Max Planck Institute for Biogeochemistry, 07745 Jena, Germany
[16]Graduate School of Bioagricultural Sciences, Nagoya University, Nagoya 464-8601, Japan
[17]Graduate School of Engineering, Osaka University, Suita 565-0871, Japan
[18]Faculty of Agriculture, Iwate University, Morioka 020-8550, Japan
[19]Kansai Research Center, Forestry and Forest Products Research Institute, Kyoto 612-0855, Japan
[20]National Institute of Advanced Industrial Science and Technology (AIST), Tsukuba 305-8569, Japan
[21]Institute of Science and Technology, Niigata University, Niigata 950-2181, Japan
[22]School of Forestry and Resource Conservation, National Taiwan University, Taipei 106319, Taiwan
[23]Sapporo Experimental Forest, Hokkaido University, Sapporo 060-0809, Japan
[24]Sustainable System Research Laboratory, Central Research Institute of Electric Power Industry, Abiko 270-1194, Japan
[25]Forestry Research Institute, Forest Research Department, Hokkaido Research Organization, Bibai 079-0198, Japan
[26]Nagoya University, Nagoya 464-8601, Japan

[27]Institute for Agro-Environmental Sciences, National Agriculture and Food Research Organization (NARO), Tsukuba 305-8604, Japan
[28]Center for Environmental and Societal Sustainability, Gifu University, Gifu 501-1193, Japan
[29]Graduate School of Agriculture, Kyoto University, Kyoto 606-8502 Japan
[30]Memuro Research Station, Hokkaido Agricultural Research Center, NARO, (HARC/M /NARO), Memuro 082-0081, Japan
[31]Institute of Life and Environmental Sciences, University of Tsukuba, Tsukuba 305-8572, Japan
[32]Field Science Center for Northern Biosphere, Hokkaido University, Toikanbetsu, 098-2943, Japan
[33]Center for Research in Isotopes and Environmental Dynamics (CRiED), University of Tsukuba, Tsukuba 305-8572, Japan
[34]Institute for Space-Earth Environmental Research, Nagoya University, Nagoya 464-8601, Japan
[35]Department of Geography, Tokyo Metropolitan University, Tokyo 192-0397 Japan
[36]Research Institute for Sustainable Humanosphere, Kyoto University, Uji 611-0011, Japan
[37]Kasuya Research Forest, Kyushu University, Fukuoka 811-2415, Japan
[38]Institute for Biological Problems of Cryolithozone, Yakutsk 677980, Russia
[39]Faculty of Engineering, Ehime University, Matsuyama 790-8577, Japan
[40]Faculty of Agriculture, Shinshu University, Nagano 399-4598, Japan
[41]Faculty of Agriculture, University of the Ryukyus, Okinawa 903-0213, Japan
[☆]retired

Correspondence: Masahito Ueyama (mueyama@omu.ac.jp)

Received: 28 December 2024 – Discussion started: 12 February 2025
Revised: 20 May 2025 – Accepted: 20 May 2025 – Published:

Abstract. Eddy covariance observations play a pivotal role in understanding the land–atmosphere exchange of energy, water, carbon dioxide (CO_2), and other trace gases, as well as the global carbon cycle and earth system. To promote the networking of individual measurements and the sharing of data, FLUXNET links regional networks of researchers studying land–atmosphere processes. JapanFlux was established in 2006 as a national branch of AsiaFlux. Despite the growing amount of shared data globally, the availability in Asia is currently limited. In this study, we developed an open dataset of the eddy covariance observations for Japan and East Asia, called JapanFlux2024, that was conducted by researchers affiliated with Japanese research institutions. The data were processed using selected standard methods from the FLUXNET community, with adaptations specific to the JapanFlux2024 dataset. Here, we present the data description and data processing and show the value of processed fluxes of sensible heat, latent heat, and CO_2. The dataset will facilitate important studies for Japan and East Asia, such as land–atmosphere interactions, improvement of process models, and upscaling fluxes using machine learning and remote sensing technology, as well as bridge collaborations between Asia and FLUXNET. TS1

1 Introduction

The global network of micrometeorological flux observations, FLUXNET (Delwiche et al., 2024; https://fluxnet.org/, last access: 27 December 2024), plays a pivotal role in multidisciplinary fields, such as land–atmosphere interactions, global biogeochemical cycles, and earth system science (Baldocchi et al., 2024; Bonan et al., 2012). FLUXNET started in 1997 as a global network of eddy covariance observations that provides data on land–atmosphere exchanges of energy, water, carbon dioxide (CO_2), methane (CH_4), and other trace gases by measuring direct turbulent transfer. The quasi-continuous eddy covariance observations revealed variations of land–atmosphere exchange at the diurnal, seasonal, interannual, and decadal scales, ranging from site (Takamura et al., 2023; Ueyama et al., 2024) to global (Beer et al., 2010; Keenan et al., 2023; Ueyama et al., 2020a) scales.

The eddy flux communities have developed publicly open databases to promote the multidisciplinary sciences. FLUXNET has periodically released the open datasets for eddy covariance observations: La Thuile Database (252 sites in 2007; Verma et al., 2014; https://fluxnet.org/data/la-thuile-dataset/, last access: 27 December 2024) and FLUXNET2015 (212 sites in 2015; Pastorello et al., 2020). Together with the global carbon project (Friedlingstein et al., 2023; https://www.globalcarbonproject.org, last access: 27 December 2024), FLUXNET also provided a topical dataset, FLUXNET-CH_4 (Delwiche et al., 2021), which promotes understanding of wetland CH_4 emissions across the globe (Knox et al., 2019; Ueyama et al., 2023). Multiple open databases for the environmental sciences have also been developed for understanding CO_2 fluxes in high-latitude ecosystems (Virkkala et al., 2022) and soil respiration (Bond-Lamberty et al., 2020).

Asia has ca. ∼ 60 % of the total world population, and thus humans have been intensively modifying forest land cover in this region for food and energy production. Such land use changes, in combination with climate change, are likely to impact the regional and global carbon and water cycling. These issues are the greatest environmental concerns for the survival of the human population. Flux studies using eddy covariance observations were conducted since the early 1990s for agricultural fields, wetlands, lakes, plantations, primary and secondary forests, disturbed ecosystems, and urban areas. In Asia, although private databases for eddy covariance measurements were developed (Hirata et al., 2008; Ichii et al., 2017; Saigusa et al., 2013), no open databases have yet been developed except the AsiaFlux database (https://asiaflux.net/, last access: 27 December 2024), which does not provide consistent gap-filling and flux partitioning.

JapanFlux (https://www.japanflux.org/, last access: 27 December 2024) was established in 2006 as a national branch of AsiaFlux (Kang and Cho, 2021; Mizoguchi et al., 2009) for the promotion of a network of micrometeorological measurements by researchers affiliated with Japanese research institutions. The mission of JapanFlux is to promote micrometeorological measurements and their collaborations with each other, researchers from other countries, and other research fields (e.g., remote sensing and modeling). Measurements by Japanese institutions have been conducted in Japan and other regions of East Asia (Mizoguchi et al., 2009; Saigusa et al., 2013) since the early 1990s for understanding energy, water, carbon, and greenhouse gas exchanges at various land surfaces.

In this study, we developed JapanFlux2024, the first publicly open dataset by JapanFlux that consists of micrometeorological data measured since the early 1990s. The data are processed with the selected standard methods employed by the FLUXNET community. The dataset is prepared with consistent post-processing, such as gap-filling and flux partitioning, and provides data at various temporal resolutions of half-hourly/hourly, daily, weekly, monthly, and annual intervals. The dataset consists of data collected at 83 sites with 683 site-years. The dataset promotes collaborations between researchers in Japan and other countries and improves our understanding of land–atmosphere interactions.

2 Data and methods

The JapanFlux2024 dataset is processed using selected standard methods from the FLUXNET community, with adaptations specific to the JapanFlux2024 dataset. According to

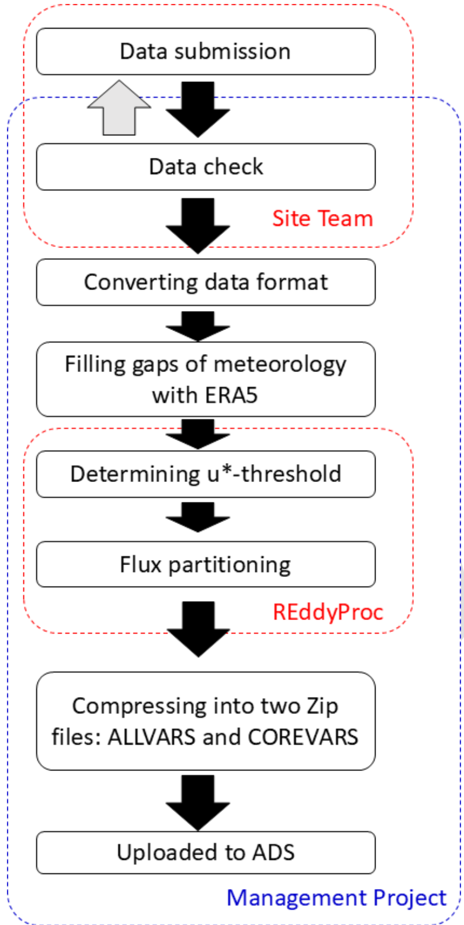

Figure 1. Flow chart of data processing in the JapanFlux2024 dataset. The details in each step and meaning of abbreviations are shown in the text.

the processing strategy of Pastorello et al. (2020), the JapanFlux2024 dataset was developed in four steps: (1) data submission by site teams, (2) formatting data in a FLUXNET format, (3) gap-filling and flux partitioning, and (4) preparing subsets and complete datasets (Fig. 1). Meta data files, so-called Biological, Ancillary, Disturbance, and Metadata (BADM), were also prepared. The data are available from the data portal (https://ads.nipr.ac.jp/japan-flux2024/, last access: 27 December 2024) under the Arctic and Antarctic Data archive System (ADS). Under the ADS, a digital object identifier (DOI) was provided for each site (Table 1). The processing pipeline mentioned in this data paper represents steps downstream of "Filling gaps in meteorology with ERA5" in Fig. 1.

2.1 Data collections

We collected the micrometeorological measurement data from the site teams, which were identified using the web pages for AsiaFlux (https://www.asiaflux.net/, last access: 11

Table 1. TS2 Information about sites included in the JapanFlux2024 dataset.

Site code (BADM)	AsiaFlux ID	Country	Country ID	Site name	Latitude (degree)	Longitude (degree)	Elevation (m)	Köppen climate	IGBP (land use)	Status	Years	Reference	Data citation
RU-Tur	TUR	Russia	RU	Tura	64.208888	100.463555	250	Dfc	DNF	Ongoing	2004	Nakai et al. (2008)	Matsuura and Morishita (2025)
RU-NeB		Russia	RU	Neleger Burnt Forest	62.325937	129.487342	221	Dfd	GRA	Completed	1999–2000	Iwahana et al. (2005)	Machimura (2025a)
RU-NeF		Russia	RU	Neleger larch forest	62.315615	129.499964	223	Dfd	DNF	Completed	1999–2006	Iwahana et al. (2005)	Machimura (2025b)
RU-NeC		Russia	RU	Neleger Cutover	62.314844	129.500075	221	Dfd	OSH	Completed	2001–2006	Iwahana et al. (2005)	Machimura (2025c)
RU-SkP	YLF	Russia	RU	Yakutsk Spasskaya Pad larch	62.25471	129.618543	217	Dfc	DNF	Ongoing	2004–2014	Ohta et al. (2008)	Maximov et al. (2025b)
RU-Sk2	YPF	Russia	RU	Yakutsk Spasskaya Pad Pine	62.241291	129.651336	216	Dfc	ENF	Completed	2004–2008	Hamada et al. (2004)	Kotani et al. (2025)
RU-USk		Russia	RU	Ulakhan Sykkhan Alas	62.150995	130.527517	143	Dfd	GRA	Completed	2000	Yabuki et al. (2004)	Yabuki et al. (2025)
RU-Ege		Russia	RU	Elgeeii forest station	60.01551563	133.8240123	203	Dfd	DNF	Ongoing	2010–2018	Kotani et al. (2014)	Maximov et al. (2025a)
MN-Skt	SKT	Mongolia	MN	Southern Khentei Taiga	48.351861	108.654333	1630	Dwc	DNF	Completed	2003–2006	Li et al. (2005b)	Asanuma (2025b)
MN-Udg		Mongolia	MN	Udleg practice forest	48.25638888	106.8511111	1342	Dwc	DNF	Ongoing	2010–2012	Miyazaki et al. (2014)	Ishikawa (2025)
MN-Nkh		Mongolia	MN	Nalaikh grassland	47.693592	107.489342	1531	BSk	GRA	Completed	2015–2020	Wang et al. (2023)	Wang et al. (2025b)
MN-Hst		Mongolia	MN	Hustai grassland	47.594131	105.856439	1227	BSk	GRA	Completed	2015–2020	Wang et al. (2023)	Wang et al. (2025a)
MN-Kbu	KBU	Mongolia	MN	Kherlenbayan Ulaan	47.213972	108.737333	1235	Bsk	GRA	Completed	2003–2009	Li et al. (2005a)	Asanuma (2025a)
CN-Lsh	LSH	China	CN	Laoshan	45.279839	127.578206	340	Cfc	DNF	Ongoing	2002–2006	Wang et al. (2005)	Saigusa and Wang (2025)
JP-Sb1		Japan	JP	Sarobetsu Mire Moss	45.104722	141.688194	6	Dfb	WET	Completed	2007–2010	Hirano et al. (2016)	Hirano (2025a)
JP-Sb2		Japan	JP	Sarobetsu Mire Sasa	45.103611	141.680833	4	Dfb	WET	Completed	2007–2010	Hirano et al. (2016)	Hirano (2025b)
JP-Tef	TSE	Japan	JP	CC-LaG Teshio Experimental Forest	45.055808	142.107122	79.47	Dfb	DNF	Ongoing	2001–2023	Takagi et al. (2009)	Takagi and Takahashi (2025)
JP-MBF	MBF	Japan	JP	Moshiri Birch Forest Site	44.38416667	142.3186111	596	Af	DBF	Completed	2003–2011	Nakai et al. (2006)	Nakai et al. (2025a)
JP-MMF	MMF	Japan	JP	Moshiri Mixd Forest Site	44.32194444	142.2613889	343	Af	MF	Completed	2003–2011	Nakai et al. (2006)	Nakai et al. (2025b)
JP-BBY	BBY	Japan	JP	Bibai bog	43.32296	141.81079	17	Dfb	WET	Completed	2012–2021	Ueyama et al. (2020c)	Ueyama et al. (2025e)
JP-Km1		Japan	JP	Kushiro Mire: Onnenai Fen	43.107511	144.330906	4.9	Dfb	WET	Completed	1994–1996, 1998	Miyata et al. (1997)	Harazono and Miyata (2025a)
JP-Km2		Japan	JP	Kushiro Mire: Akanuma Bog	43.1	144.35	7	Dfb	WET	Completed	1998–1999	Miyata et al. (2001)	Harazono and Miyata (2025b)
JP-Spp	SAP	Japan	JP	Sapporo forest meteorology research site	42.9868431	141.3853305	174	Dfb	DBF	Ongoing	2000–2018	Yamanoi et al. (2015)	Mizoguchi and Kitamura (2025)
CN-In4		China	CN	Inner Mongolia maize	42.94413333	120.7266222	354	Bsk	CRO	Completed	1994	Li et al. (2000)	Harazono and Takagi (2025d)
CN-In5		China	CN	Inner Mongolia no grazing	42.93415833	120.7090778	355	Bsk	GRA	Completed	1992–1994	Li et al. (2000)	Harazono and Takagi (2025e)
CN-In6		China	CN	Inner Mongolia heavy grazing	42.93401389	120.7115472	355	Bsk	GRA	Completed	1992–1994	Li et al. (2000)	Harazono and Takagi (2025f)
CN-In8		China	CN	Inner Mongolia medium grazing	42.93396667	120.7105306	355	Bsk	GRA	Completed	1992, 1994	Li et al. (2000)	Harazono and Takagi (2025h)
CN-In2		China	CN	Inner Mongolia grassland	42.93396389	120.7109639	355	Bsk	GRA	Completed	1991	Li et al. (2000)	Harazono and Takagi (2025b)
CN-In7		China	CN	Inner Mongolia light grazing	42.93391944	120.7096056	355	Bsk	GRA	Completed	1992–1994	Li et al. (2000)	Harazono and Takagi (2025g)
CN-In1		China	CN	Inner Mongolia dune	42.92970833	120.70735	356	Bsk	BSV	Completed	1990–1991	Li et al. (2000)	Harazono and Takagi (2025a)
CN-In3		China	CN	Inner Mongolia soybean	42.94413333	120.7266222	354	Bsk	CRO	Completed	1994	Li et al. (2000)	Harazono and Takagi (2025c)

Table 1. Continued.

Site code (BADM)	AsiaFlux ID	Country	Country ID	Site name	Latitude (degree)	Longitude (degree)	Elevation (m)	Köppen climate	IGBP (land use)	Status	Years	Reference	Data citation
JP-Tmk	TMK	Japan	JP	Tomakomai Flux Research Site	42.736972	141.516944	140	Dfb	DNF	Completed	2001–2003	Hirano et al. (2003)	Hirata and Hirano (2025)
JP-Tmd	TMK	Japan	JP	Tomakomai Flux Research Site Disturbed	42.735911	141.523147	117	Dfb	DBF	Ongoing	2005–2023	Hirano et al. (2017)	Hirano and Hirata (2025)
JP-Toc		Japan	JP	Tomakomai Crane site	42.709727	141.565898	96	Dfb	DBF	Ongoing	2010–2014	Nakamura et al. (2014)	Nakaji et al. (2025)
JP-Tom	TOE	Japan	JP	Tomakomai Experimental Forest	42.698906	141.571488	90	Dfb	DBF	Completed	1999–2013	Shibata et al. (2005)	Nakaji (2025)
JP-Srk	SRK	Japan	JP	Shirakami Beech Forest Site	40.565485	140.127794	340	Dfa	DBF	Ongoing	2010–2016	Ishida et al. (2009)	Ishida (2025)
JP-Api	API	Japan	JP	Appi forest meteorology research site	40.0013585815243	140.936585918296	831	Dfa	DBF	Ongoing	2000–2022	Yasuda et al. (2012)	Yasuda (2025a)
JP-Mra	MRA	Japan	JP	Muramatsu Agricultural Field	37.690275	139.194429	43	Cfa	CRO	Ongoing	2023	Boiarskii and Hasegawa (2019)	Nagano and Hasegawa (2025)
CN-HaM	QHB	China	CN	Qinghai Flux Research Site	37.607432	101.332	3250	BSk	GRA	Ongoing	2001–2014	Du et al. (2021)	Du et al. (2025)
JP-NsM	NSS	Japan	JP	Nasu Research Station, Manure Application Plot	36.91583333	139.9358333	320	Cfa	GRA	Completed	2004–2015	Matsuura et al. (2023)	Matsuura (2025a)
JP-NsC	NSS	Japan	JP	Nasu Research Station, Chemical Fertilizer Plot	36.915	139.9366667	320	Cfa	GRA	Completed	2004–2015	Matsuura et al. (2023)	Matsuura (2025b)
JP-Kzw	KZW	Japan	JP	Karuizawa	36.406667	138.5725	1385	Dfb	DBF	Completed	2001–2008	Nakaya et al. (2006)	Nakaya et al. (2025)
JP-Tkb		Japan	JP	Tsukuba Experimental Watershed	36.173379	140.176634	341	Cfa	ENF	Ongoing	2014, 2018–2021	Iida et al. (2020)	Shimizu et al. (2025b)
JP-Tak	TKY	Japan	JP	Takayama deciduous broadleaf forest site	36.14616667	137.4231111	1425	Dfb	DBF	Ongoing	1998–2021	Murayama et al. (2024a)	Murayama et al. (2025b)
JP-Ta2	TKC	Japan	JP	Takayama evergreen coniferous forest site	36.139722	137.370833	800	Dfb	ENF	Ongoing	2005–2022	Saitoh et al. (2010)	Saitoh and Tamagawa (2025)
JP-Tgf	TGF	Japan	JP	Terrestrial Environment Research Center, University of Tsukuba	36.11353	140.09488	27	Cfa	GRA	Completed	2002–2022	Shimoda et al. (2005)	Asanuma and Shimoda (2025)
JP-KaP		Japan		Kasumigaura lotus paddy	36.08	140.24	3	Cfa	CRO	Completed	1997–1998	Takagi et al. (2003)	Harazono et al. (2025)
JP-Mse	MSE	Japan	JP	Mase paddy flux site	36.05393	140.02693	11	Cfa	CRO	Ongoing	2001–2009	Saito et al. (2005)	Ono (2025)
JP-SwL	SWL	Japan	JP	Suwa Lake Site	36.04657222	138.1083528	758	Dfc	WAT	Ongoing	2015–2023	Iwata et al. (2018)	Iwata (2025b)
JP-KaL		Japan	JP	Koshin, Lake Kasumigaura	36.037778	140.404167	0.26 (at the water level of Y.P.1.1 m)	Cfa	WAT	Ongoing	2007–2022	Sugita et al. (2020)	Sugita (2025)
JP-Nsb		Japan	JP	NIAES Soybean	36.024303	140.114975	24	Cfa	CRO	Completed	1990	Harazono et al. (1992)	Harazono (2025a)
JP-Yrp		Japan	JP	Yawara Rice paddy	36.00766667	140.0301752	23	Cfa	CRO	Completed	1993–1995	NA	Harazono (2025b)
JP-Kwg	KWG	Japan	JP	Kawagoe forest meteorology research site	35.8725	139.4869	41	Cfa	DBF	Completed	1997–2002	Yasuda et al. (1998)	Yasuda (2025b)
JP-Shn		Japan	JP	Shinshu University Experimental Forest Site	35.865755	137.932563	775	Dfa	MF	Ongoing	2014–2019	NA	Iwata and Suzuki (2025)
JP-Nkm	NKM	Japan	JP	Nishikoma Site	35.808064	137.833883	2641	Dfb	ENF	Ongoing	2018–2023	NA	Iwata (2025a)
JP-Fmt		Japan	JP	Field Museum Tama Hills	35.638745	139.379748	168	Cfa	MF	Ongoing	2013–2023	Matsuda et al. (2015)	Takagi and Matsuda (2025)
JP-Kgu		Japan	JP	Kugahara urban residential area	35.582859	139.693543	18.5	Cfa	URB	Completed	2001–2002	Moriwaki and Kanda (2004)	Kanda and Moriwaki (2025)
JP-Fjy	FJY	Japan	JP	Fujiyoshida forest meteorology research site	35.45454	138.76225	1043	Cfa	ENF	Ongoing	2000–2021	Mizoguchi et al. (2012)	Takanashi et al. (2025a)

Table 1. Continued.

Site code (BADM)	AsiaFlux ID	Country	Country ID	Site name	Latitude (degree)	Longitude (degree)	Elevation (m)	Köppen climate	IGBP (land use)	Status	Years	Reference	Data citation
JP-Fhk	FHK	Japan	JP	Fuji Hokuroku Flux Observation Site	35.44355577	138.7646931	1100	Cfa	DNF	Ongoing	2006–2023	Takahashi et al. (2015)	Takahashi et al. (2025)
JP-Hrt		Japan	JP	Hiratsuka Rice Paddy	35.362778	139.338056	6.98	Cfa	CRO	Completed	2013	Komiya (2015)	Komiya (2025a)
JP-SMF	SMF	Japan	JP	Seto Mixed Forest Site	35.261528	137.07875	212	Cfa	MF	Completed	2002–2016	Matsumoto et al. (2008)	Kotani and Ohta (2025)
JP-Nuf		Japan	JP	Nagoya University Forest	35.15241667	136.9718889	66	Cfa	DBF	Completed	2000–2001	Hiyama et al. (2005)	Awal and Ohta (2025a)
JP-Tdf		Japan	JP	Toyota Deciduous Forest	35.03588889	137.1857778	104	Cfa	DBF	Completed	2002–2004	Awal et al. (2010)	Awal and Ohta (2025b)
JP-Yms	YMS	Japan	JP	Yamashiro forest meteorology research site	34.790278	135.840939	220	Cfa	DBF	Ongoing	2000–2023	Kominami et al. (2008)	Takanashi et al. (2025b)
JP-Nap		Japan	JP	Nunoike Agricultural Pond	34.77485	134.892442	40	Cfa	WAT	Completed	2021–2023	NA	Sakabe and Itoh (2025)
JP-Ako	AKO	Japan	JP	Akou green belt	34.735192	134.374798	10.5	Cfa	EBF	Completed	2000–2003	Kosugi et al. (2005)	Kosugi and Takanashi (2025)
JP-Sac	SAC	Japan	JP	Sakai City Office	34.57391389	135.4828889	17	Cfa	URB	Ongoing	2008–2023	Ueyama and Takano (2022)	Ueyama (2025d)
JP-Ozm	IZM	Japan	JP	Oizumi Urban Park	34.563469	135.533483	22	Cfa	URB	Completed	2015–2016	Ueyama and Ando (2016)	Ueyama (2025a)
JP-Om1	OM1	Japan	JP	B11 building in Osaka Metropolitan University	34.547177	135.502861	27	Cfa	URB	Ongoing	2014–2023	Ueyama and Ando (2016)	Ueyama (2025b)
JP-Om2	OM2	Japan	JP	Farm field in Osaka Metropolitan University	34.542452	135.508227	50	Cfa	GRA	Ongoing	2022–2023	NA	Ueyama (2025c)
JP-Hc3		Japan	JP	Hachihama Experimental Farm: Double Crop	34.539672	133.911731	−0.25	Cfa	CRO	Completed	2005–2009	Takimoto et al. (2010)	Takimoto and Iwata (2025b)
JP-Hc1		Japan	JP	Hachihama Experimental Farm: the International Rice Experiment	34.53789167	133.9267972	0	Cfa	CRO	Completed	1996	Harazono et al. (1998)	Harazono (2025c)
JP-Hc2	HCH	Japan	JP	Hachihama Experimental Farm	34.537518	133.927545	−1	Cfa	CRO	Completed	1999–2008	Ohtaki (1984)	Takimoto and Iwata (2025a)
JP-Khw	KHW	Japan	JP	Kahoku Experiment watershed	33.13658	130.70834	196	Cfa	ENF	Ongoing	2000–2003, 2007–2021	Shimizu et al. (2015)	Kitamura et al. (2025)
JP-Ynf	YNF	Japan	JP	Yona-Field Tower Site	26.751	128.212667	213	Cfa	EBF	Ongoing	2013–2022	Matsumoto et al. (2023)	Matsumoto et al. (2025)
TH-Kog		Thailand	TH	Kog-Ma Watershed	18.8	98.9	1265	Af	EBF	Completed	2005–2013	Kume et al. (2007)	Kumagai and Takamura (2025a)
TH-Mae		Thailand	TH	Mae Moh plantation	18.38333333	99.71666667	380	Aw	DBF	Completed	2005–2016	Igarashi et al. (2015)	Kumagai and Takamura (2025b)
TH-Kms		Thailand	TH	Kamphaeng Saen Rice Paddy	14.009167	99.984167	4.74	Aw	CRO	Completed	2014	Komiya (2015)	Komiya (2025b)
KH-Kmp		Cambodia	KH	Kampong Thom Lowland Dry Evergreen Forest	12.74457978	105.4785661	95	Am	EBF	Ongoing	2011–2014	Kabeya et al. (2021)	Shimizu et al. (2025a)
MY-LHP	LHP	Malaysia	MY	Lambir Hills National Park	4.201007	114.039079	140	Af	EBF	Completed	2009–2019	Takamura et al. (2023)	Kumagai et al. (2025)
ID-Pag		Indonesia	ID	Palangkaraya Undrained Forest	−2.323916667	113.9043917	22	Am	EBF	Ongoing	2004–2019	Hirano et al. (2024)	Hirano and Ohkubo (2025c)
ID-PaB		Indonesia	ID	Palangkaraya Drained Burnt forest	−2.340796	114.0379	14	Am	OSH	Completed	2004–2017	Ohkubo et al. (2021)	Hirano and Ohkubo (2025a)
ID-PaD	PDF	Indonesia	ID	Palangkaraya Drained forest	−2.346070697	114.036408	26	Am	EBF	Completed	2001–2017	Hirano et al. (2024)	Hirano and Ohkubo (2025b)

NA: not available.

July 2024) and JapanFlux (https://www.japanflux.org/, last access: 11 July 2024). We also collected information on previous studies that reported micrometeorological measurements from domestic researcher connections and literature surveys. The collected data were from eddy covariance observations that were carried out by site teams affiliated with Japanese research institutes and universities. By this criterion, the dataset covers not only Japan but also other countries, such as Russia, China, Mongolia, Cambodia, Thailand, Malaysia, and Indonesia. Most of the sites were established for long-term monitoring of CO_2 fluxes, but intensive observations for about a week in the 1990s were also included in the dataset. Because the data format differed for each team, we reformatted the file to the FLUXNET format (https://ameriflux.lbl.gov/data/aboutdata/data-variables/, last access: 11 July 2024) after consultation with each site team. Generally, non-gap-filled data were provided by the site teams, but some teams provided gap-filled meteorological and flux data in addition to the non-gap-filled data. The JapanFlux2024 dataset differs from datasets such as FLUXNET2015 in that it provides site principal investigators (PIs), with increased flexibility in data screening. When clear anomalies were identified, quality control procedures were applied by the management team in collaboration with the respective site PI.

The dataset consists of data from 83 sites with 683 site-years, of which 52 sites are located in Japan (Fig. 2; Table 1). The dataset includes 43 forest sites, 15 grassland sites, 5 wetland sites, 10 cropland sites, 3 lake and pond sites, and 4 sites in urban landscapes. Sites that suffered from various types of disturbance are also included: wind damage by typhoon (JP-Tmd, JP-Spp), fire (RU-NeB, ID-PaB), harvesting (RU-NeC, JP-Tef), thinning (JP-Fhk), insect outbreak (JP-Api), drainage (ID-Pag), and mowing (JP-NsC, JP-NsM, JP-Tgf, JP-Om2). The data records started in 1990 at a soybean cropland in Japan (Harazono et al., 1992), increased in number in the early 2000s, and peaked at 34 sites in 2008, 2014, and 2015 (Fig. 3). More recently, the number of data records gradually declined owing to site closure or the fact that the data have not been processed yet. The longest record was 24 years (JP-Tak and JP-Yms; both deciduous broadleaf forests) (Fig. 4). There are 26 sites with observation records of CO_2 flux for more than 10 years and six sites with those for more than 20 years (JP-Tef, JP-Tmk/JP-Tmd, JP-Api, JP-Fjy, JP-Tak, JP-Yms). Note that JP-Tmk and JP-Tmd represent a continuous observation series, although they are assigned different site IDs. At 12 sites, data records are available for less than 1 year. Data for CH_4 flux are available at six sites (JP-BBY, JP-SwL, JP-Nap, JP-Hrt, JP-Sac, JP-Om1).

2.2 Gap-filling meteorological variables

As with the FLUXNET2015 dataset (Pastorello et al., 2020; Vuichard and Papale, 2015), the meteorological variables were filled using the European Center for Medium-Range Weather Forecasts Reanalysis v5 (ERA5) data (Hersbach et al., 2020). Instead of using ERA5, we used the gap-filled meteorology if the site teams had filled the gaps. If meteorological variables for multiple sensors or positions were available, these variables were prioritized and aggregated; if data were missing in the highest-priority dataset, they were filled with values from the second-highest-priority dataset or, if that were also unavailable, based on the priority order. The gaps in the aggregated meteorological variables were then filled with ERA5 data because measured variables were less biased than ERA5, even when measured at different locations within a site. Air temperature, relative humidity, wind speed, downward shortwave radiation, downward longwave radiation, precipitation, and atmospheric pressure were filled using ERA5 after correcting biases at each site for each year. Linear regression for meteorological variables (except precipitation) between observations and ERA5 was determined and then applied to correct site-specific biases in ERA5 to fill the data gaps. Water vapor pressure was calculated from the relative humidity, and the gaps in relative humidity were filled using the gap-filled water vapor pressure and air temperature rather than directly using the relative humidity. If all meteorological variables were missing in some years when constructing the linear regression, the bias was corrected using a regression for the entire multi-year data record. For precipitation (denoting rainfall plus snowfall), we determined the ratio of the annual precipitation between observations and ERA5 during the period when observed precipitation were available and then filled hourly or half-hourly precipitation after multiplying the ERA5-based precipitation by the ratio. If only the rainfall was measured, the correction ratio was determined using liquid precipitation, which was defined as precipitation when the relative humidity was below the critical relative humidity (RH_{cri}; %): $RH_{cri} = 92.5–7.5T$, where T is the air temperature (Matsuo and Sasyo, 1981).

2.3 Gap-filling and flux partitioning

Gap-filling and flux partitioning were conducted based on REddyProc (version 1.3.2; Wutzler et al., 2018). First, the friction velocity (u^*) threshold was determined for the identified low-turbulence conditions during the nighttime using the moving-point method (Papale et al., 2006). The u^* threshold was determined from the temperature sensitivity of nighttime net ecosystem exchange (NEE) by seasonal clustering, an approach that is widely used in the FLUXNET community. In the moving point method, the u^* threshold was first determined for each of the four seasons, and the maximum value among them was used for the entire year. Thus, the determined u^* threshold was conservative (Papale et al., 2006). In this dataset, we determined the u^* threshold for each year to consider its potential shift over the years, which is termed as a variable u^* threshold (vUT). The vUT differs slightly from the definition of the variable u^* threshold (VUT) in FLUXNET2015 (Pastorello et al., 2020) (Table 2):

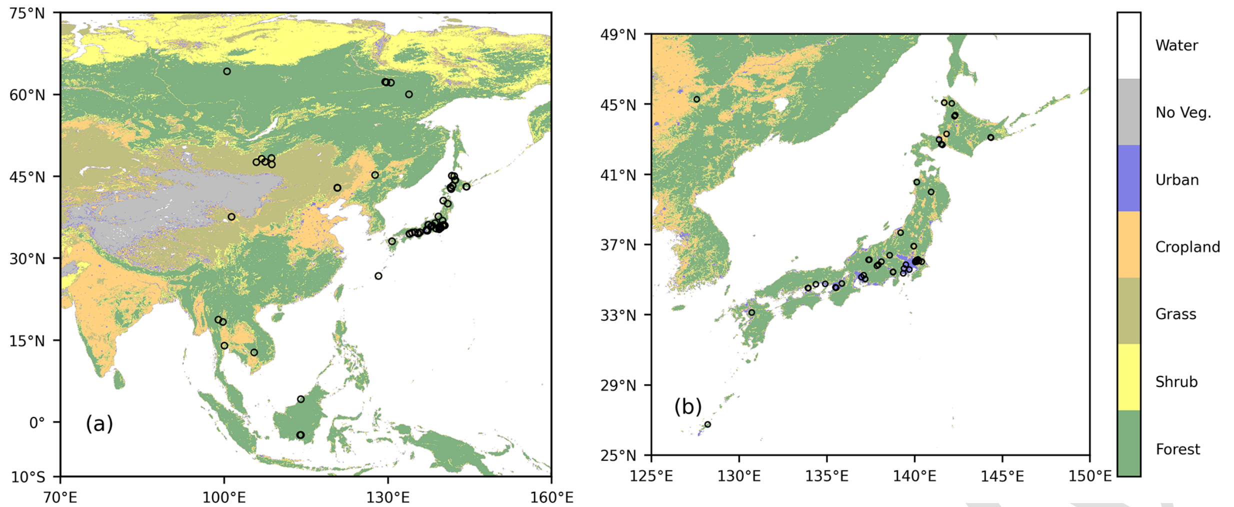

Figure 2. Distributions of the sites that constitute the JapanFlux2024 database on a land cover map provided by the MOD12 product (version 6.1; Sulla-Menashe et al., 2019): a map of the Asia region **(a)** and an enlarged map showing Japan **(b)**.

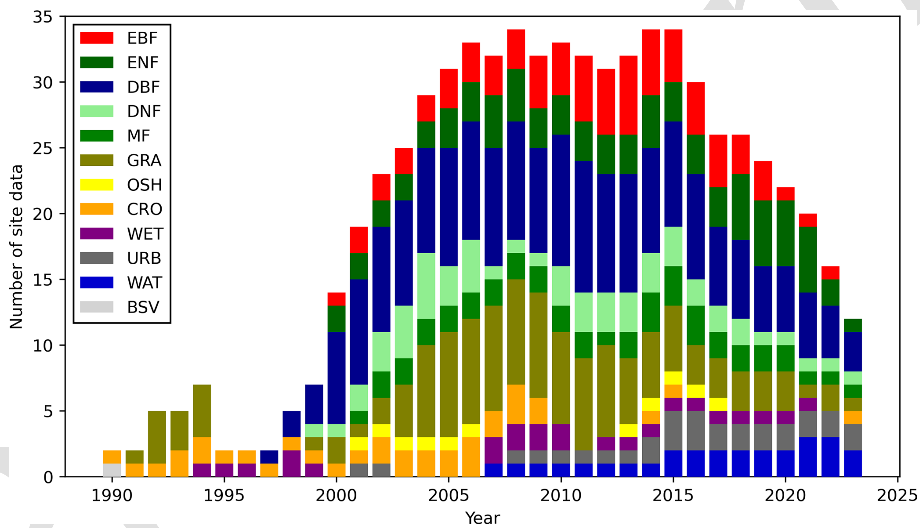

Figure 3. Number of site data records for each year. Land cover types: evergreen broadleaf forest (EBF), evergreen needleleaf forest (ENF), deciduous broadleaf forest (DBF), deciduous needleleaf forest (DNF), mixed forest (MF), grassland (GRA), open shrubland (OSH), cropland (CRO), wetland (WET), urban (URB), lake (WAT), and barren sparse vegetation (BSV).

the VUT in FLUXNET2015 was determined by pooling data from each year along with data from the immediately preceding and following years (if available). The u^* threshold was determined with 100 bootstrap replicates, where reference (original data obtained without using a bootstrapped sample) and the 5th, 50th, and 95th percentiles of the estimated u^* threshold were used for subsequent data filtering, gap-filling, and flux partitioning. Here, the nighttime was defined as downward shortwave radiation $< 10\,\mathrm{W\,m^{-2}}$ and was further confirmed using exact solar time at the site location. On the basis of the estimated u^* threshold, nighttime CO_2 fluxes and/or NEE were eliminated. This dataset does not include the estimation of NEE using the constant u^* threshold (CUT) nor the advanced uncertainty estimation provided with the _REF suffix, as implemented in the ONEFLUX pipeline (Pastorello et al., 2020). For urban sites, the threshold was generally not used for two reasons (e.g., Liu et al., 2012; Ueyama and Ando, 2016): (1) nighttime CO_2 fluxes were not expected to correlate with air temperature, making it difficult to evaluate the correct u^* threshold, and (2) the surface layer was often unstable, even at night. Consequently, the u^* filtering was not applied for highly urbanized sites (JP-Sac and JP-Kgu).

Gaps in sensible heat flux (H), latent heat flux (LE), and NEE were filled using marginal distribution sampling (MDS) based on REddyProc. In MDS, a lookup table (LUT) with

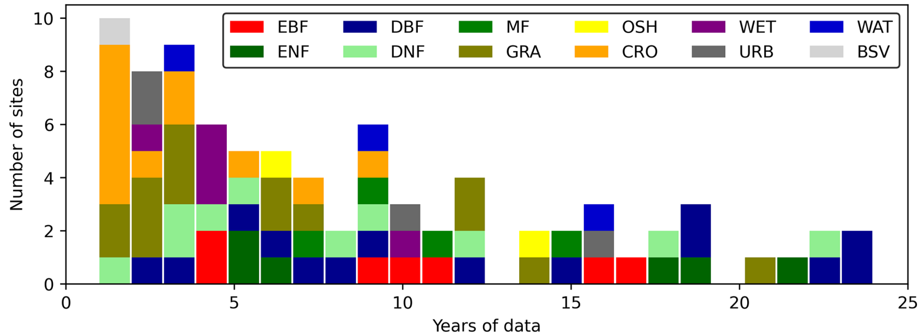

Figure 4. Number of site records for different durations of data records. Sites affected by a disturbance that changed the vegetation type during the observational period were classified according to the dominant land cover type: JP-Tef as DNF, JP-Tmd as DBF, and ID-PaB as OSH. Land cover type abbreviations are as in Fig. 3.

air temperature, downward shortwave radiation, and vapor pressure deficit (VPD) was created for a 7 d window. When data gaps could not be filled with this window, they were filled in the following order: (1) LUT was applied with a 14 d window, (2) the mean diurnal variation method (Falge et al., 2001) was applied with a 1 or 2 d window, and (3) LUT was applied with a 21 d window, which was increased with a 7 d step until reaching a 70 d window if not enough data points were available. NEE were filled using MDS with the four different u^* thresholds (reference, 5th, 50th, and 90th percentiles values), whereas H and LE were filled without applying the u^* threshold. In addition to the fluxes, net radiation, soil temperature, ground heat flux, and photosynthetic photon flux density (PPFD) were also filled using MDS. In the data collected from the site teams, energy imbalance correction (Twine et al., 2000) was not applied for H and LE at any sites; thus, the gap-filled H and LE were not corrected for the energy balance closure.

Using REddyProc, NEE was partitioned into gross primary productivity (GPP) and ecosystem respiration (RECO) using two methods: nighttime flux partitioning and daytime flux partitioning. In the nighttime partitioning method, nighttime NEE was parameterized on the basis of the temperature response function (Lloyd and Taylor, 1994) with a 7 d window, and then this function was used to calculate daytime and nighttime RECO. GPP was determined by subtracting RECO from NEE. In the daytime partitioning method (Lasslop et al., 2010), the common rectangular hyperbolic light-response curve was determined with a 4 d window, where the function accounted for the VPD effect on the initial slope of the light-response curve and the temperature effect of respiration. GPP and RECO using the daytime partitioning method were calculated based on a fitted model that combines a light-response curve and a temperature-dependent respiration model; thus, the daytime method did not directly add up the observed NEE (Wutzler et al., 2018). Using the two methods, fluxes were partitioned for NEE with different u^* thresholds.

2.4 Site-specific considerations

For the sites with heterogeneous land surfaces – JP-Khw and JP-Ozm – the dominant land surface fluxes were extracted using wind sectors. JP-Khw is an evergreen needleleaf plantation forest consisting of *Cryptomeria japonica* (sugi) and *Chamaecyparis obtusa* (hinoki), but evergreen or deciduous broadleaf trees grow in gaps in some wind sectors. The H, LE, and CO_2 fluxes for sugi, which occupies the dominant wind sector area (the right-bank side), were extracted as quality control with footprint, "_QC_FP" (Table 2). To extract these flux data, daytime fluxes for a wind sector on the right bank were selected, but nighttime fluxes for all wind sectors were used to increase data availability because there were no clear differences in nighttime fluxes among wind sectors. Gap-filling and flux partitioning were done only for the extracted data. JP-Ozm is located at the edge of an urban park; thus, measured flux representing this park (Ueyama and Ando, 2016) were selected and designated "_QC_FP" in addition to the variables for measured fluxes representing both sectors of the urban park and other land covers. Gap-filling and flux partitioning were done only for the extracted data, which represented the urban park. These extracted flux data ("_QC_FP") were included in the ALLVARS files (described in Sect. 2.5) in addition to measured fluxes for all sectors, and the gap-filled extracted fluxes were included in the COREVARS files (described in Sect. 2.5).

Flux partitioning and gap-filling for JP-Nkm, located on a complex mountainous terrain, were conducted using slope-normal shortwave radiation instead of downward shortwave radiation. Horizontally observed incident shortwave radiation was converted to radiation normal to the slope on the basis of the tilt and azimuth angles of the slope and the solar altitude and azimuth angles (Hammerle et al., 2007; Nie et al., 1992) as follows. Horizontally observed incident shortwave radiation was partitioned into direct and diffuse components using the observed diffuse fraction (BF5, Delta-T Devices, UK), and the direct component was converted to that normal to the slope surface. The diffuse component was

Table 2. List of variable base names not used in FLUXNET2015, along with their descriptions and related sites.

Base name	Description	Sites
Preprocessing variables		
SW_IN_SLOPE_PI	Slope-normal incoming shortwave radiation	JP-Nkm
NETRAD_SLOPE_PI	Slope-normal net radiation	JP-Nkm
USTAR_QC_FP	Friction velocity qualified with footprint	JP-Ozm
H_QC_FP	Sensible heat flux qualified with footprint	JP-Ozm, JP-Khw
LE_QC_FP	Latent heat flux qualified with footprint	JP-Ozm, JP-Khw
FC_QC_FP	CO_2 flux qualified with footprint	JP-Ozm, JP-Khw, JP-Sac
NEE_QC_FP	NEE flux qualified with footprint	JP-Khw
Post-processing variables		
TA_multiple	Air temperature by multiple sensors or positions	CN-In1, CN-In2, CN-In3, CN-In4, CN-In5, CN-In6, CN-In7, CN-In8, CN-Lsh, JP-BBY, JP-Fhk, JP-Fjy, JP-Hc1, JP-Ozm, JP-Khw, JP-KaP, JP-Km1, JP-Km2, JP-Kzw, JP-MBF, JP-MMF, JP-Nsb, JP-Nuf, JP-Spp, JP-Tgf, JP-Tak, JP-Tmk, JP-Tef, JP-Ynf, JP-Yrp, MN-Udg, MY-LHP, RU-Ege, RU-SkP, RU-Sk2, TH-Kog, TH-Mae, RU-USk
RH_multiple	Relative humidity by multiple sensors or positions	CN-In1, CN-In2, CN-In3, CN-In4, CN-In5, CN-In6, CN-In7, CN-In8, CN-Lsh, JP-BBY, JP-Fhk, JP-Fjy, JP-Hc1, JP-KaP, JP-Km1, JP-Km2, JP-Kzw, JP-MBF, JP-MMF, JP-Nsb, JP-Nuf, JP-Spp, JP-Tgf, JP-Tak, JP-Tmk, JP-Tef, JP-Ynf, JP-Yrp, MN-Udg, MY-LHP, RU-Ege, RU-SkP, RU-Sk2, TH-Mae, RU-USk
SW_IN_multiple	Incoming shortwave radiation by multiple sensors or positions	JP-Fhk, JP-Spp, JP-Tgf, JP-Tmk, JP-Tef, JP-Ynf
P_multiple	Precipitation by multiple sensors or positions	JP-BBY, JP-Khw
WS_IN_multiple	Wind speed by multiple sensors or positions	CN-In1, CN-In2, CN-In3, CN-In4, CN-In5, CN-In6, CN-In7, CN-In8, CN-HaM, JP-Fhk, JP-Hc1, JP-KaP, JP-Km1, JP-Km2, JP-Kzw, JP-MBF, JP-MMF, JP-Nsb, JP-Spp, JP-SMF, JP-Tgf, JP-Tef, JP-Yms, JP-Ynf, JP-Yrp, MN-Udg, TH-Kog, TH-Mae, RU-USk
G_multiple	Ground heat flux by multiple sensors or positions	JP-Sac, JP-Spp, JP-Ynf, MN-Udg
NETRAD_F_MDS	Net radiation filled with MDS	JP-Tef
PPFD_IN_F_MDS	PPFD filled with MDS	CN-Lsh, CN-HaM, JP-Km2, JP-MBF, JP-MMF, JP-Nkm, JP-Tgf, RU-SkP, TH-Kog
NEE_vUT	Gap-filled NEE with the variable u^* threshold	ALL sites
RECO_NT_vUT	RECO with the variable u^* threshold based on the nighttime approach	ALL sites
GPP_NT_vUT	GPP with the variable u^* threshold based on the nighttime approach	ALL sites
RECO_DT_vUT	RECO with the variable u^* threshold based on the daytime approach	ALL sites
GPP_DT_vUT	GPP with the variable u^* threshold based on the daytime approach	ALL sites

assumed to be isotropic. The total incident shortwave radiation normal to the slope surface was calculated as the sum of the direct component converted as above and the original diffuse component. When the diffuse fraction was not observed, it was estimated from the relationship between the diffuse fraction and cloudiness; the latter was defined as the ratio of observed incident shortwave radiation to extraterrestrial radiation (Wang et al., 2018). The slope-normal shortwave radiation was included as a variable, SW_IN_SLOPE_PI_ 1_ 1_1, in ALLVARS.

For tropical ecosystems (TH-Kms, TH-Kog, TH-Mae, ML-LHP, ID-PaB), nighttime-based flux partitioning failed because little seasonality in temperature hampered the determination of a significant relationship between nighttime CO_2 flux and temperature. For these sites, only daytime partitioning was provided in the dataset. In a subtropical forest (KH-Kmp), the determination of the u^* threshold failed; thus, the u^* threshold was estimated using gap-filled u^* by the site team instead of measured u^* with data gaps. Because the data quality of u^* for KH-Kmp seemed reasonable, we were unable to find out why REddyProc failed to determine the u^* thresholds with measured u^* in KH-Kmp. The u^* threshold for ID-Pag and ID-PaD could not be determined for several years; hence, constant u^* thresholds across these years were determined with REddyProc and applied for the subsequent data processing.

Low availability of nighttime data due to the limited fetch in JP-Ako (Kosugi et al., 2005) hampered determination of the u^* threshold, gap-filling flux for CO_2 flux, and flux partitioning with REddyProc. Consequently, no aggregated fluxes longer than half-hourly data for CO_2 flux, GPP, and RECO were provided in the dataset.

Fluxes were not partitioned for lakes and a pond (JP-SwL, JP-KaL, JP-Nap) and for an urban center (JP-Sac). For the lakes and pond, gap-filling H, LE, and CO_2 flux was based on MDS. For JP-Sac, gap-filling for H and LE was also based on MDS, but MDS was not applied to CO_2 flux because it was controlled by traffic volume and air temperature (Ueyama and Takano, 2022TS3). Gap-filling for CO_2 flux at JP-Sac was conducted by the site team on the basis of random forest regression (Ueyama and Takano, 2022) and was included as FCO2_F_PI in COREVARS and ALLVARS. The u^* threshold was not applied for JP-Nap because the moving point method (Papale et al., 2006) developed for terrestrial ecosystems was not applicable to the pond.

In this dataset, CH_4 fluxes were not gap-filled because (1) consistent gap-filling was not possible because of missing important variables, such as water table depth, and (2) inconsistent processes control CH_4 emissions on different land surfaces, such as a rice paddy (JP-Hrt), bog (JP-BBY; Ueyama et al., 2020c, b), lake (JP-SwL; Iwata et al., 2018), pond (JP-Nap), and urban landscapes (JP-Sac, JP-Om1; Takano and Ueyama, 2021). If the gap-filled CH_4 fluxes were provided by the site team (i.e., JP-BBY), the data were included as FCH4_F_PI in COREVARS; otherwise, non-gap-filled data were included in ALLVARS.

2.5 Data format

The dataset was prepared in a format partially compatible with the FLUXNET format, although the content and split of variables between ALLVARS and COREVARS were slightly different from FLUXNET2015 (Pastorello et al., 2020) (Table 2), which consists of files separated by sites, temporal aggregation (i.e., half-hourly/hourly, daily, weekly, monthly, and annual), and the data product, i.e., ALLVARS and COREVARS, as described later. The separated files for ALLVARS and COREVARS were combined into two zip files for each site.

The following file naming rules (Pastorello et al., 2020) were followed: [SITE_ID]_JapanFlux2024_[DATA_PRODUCT]_[RESOLUTION]_[FIRST_YEAR]-[LAST_YEAR]_[SITE_VERSION]-[CODE_VERSION].csv.

[SITE_ID] is the site ID. For the CC-SSS format, CC is a two-letter country code, and SSS is the three-character site code. [Data_PRODUCT] represents the data types: ALLVARS, COREVARS, AUXMETEO, AUXNEE, or ERA5. COREVARS is the data type representing selected data variables, including basic micrometeorological data and fluxes, and quality information flags. ALLVARS is a data file representing all variables of data products, including variables listed in COREVARS, original data before the processing pipeline, and internal variables. AUXMETEO includes auxiliary variables related to the meteorological downscaling of ERA5. ERA5 includes the meteorological data from ERA5 for 1990–2024. [RESOLUTION] is the temporal resolution of the data products: HH (half-hourly time step), HR (hourly time step), DD (daily time step), WW (weekly time step), MM (monthly time step), and YY (annual time step). [FIRST_YEAR] is the first year in the file, and [LAST_YEAR] is the last year in the file. The first and last years are based on the years in which the micrometeorological measurements were conducted, except for ERA5, where the first year is 1990 and the last year is 2024 for all sites. [SITE_VERSION] is the version of the original dataset, and [CODE_VERSION] is the code of the data processing pipeline used to process the dataset.

The COREVARS file included variables for basic meteorology and turbulent fluxes. The gap-filled meteorological variables of air temperature, incoming shortwave radiation, incoming longwave radiation, relative humidity, VPD, atmospheric pressure, precipitation, wind speed, net radiation, ground heat flux, soil temperature, PPFD, CO_2 concentration, soil water content, and potential shortwave radiation (top of atmosphere) were included. If the original data provided by a site team included wind direction, outgoing shortwave radiation, outgoing longwave radiation, outgoing

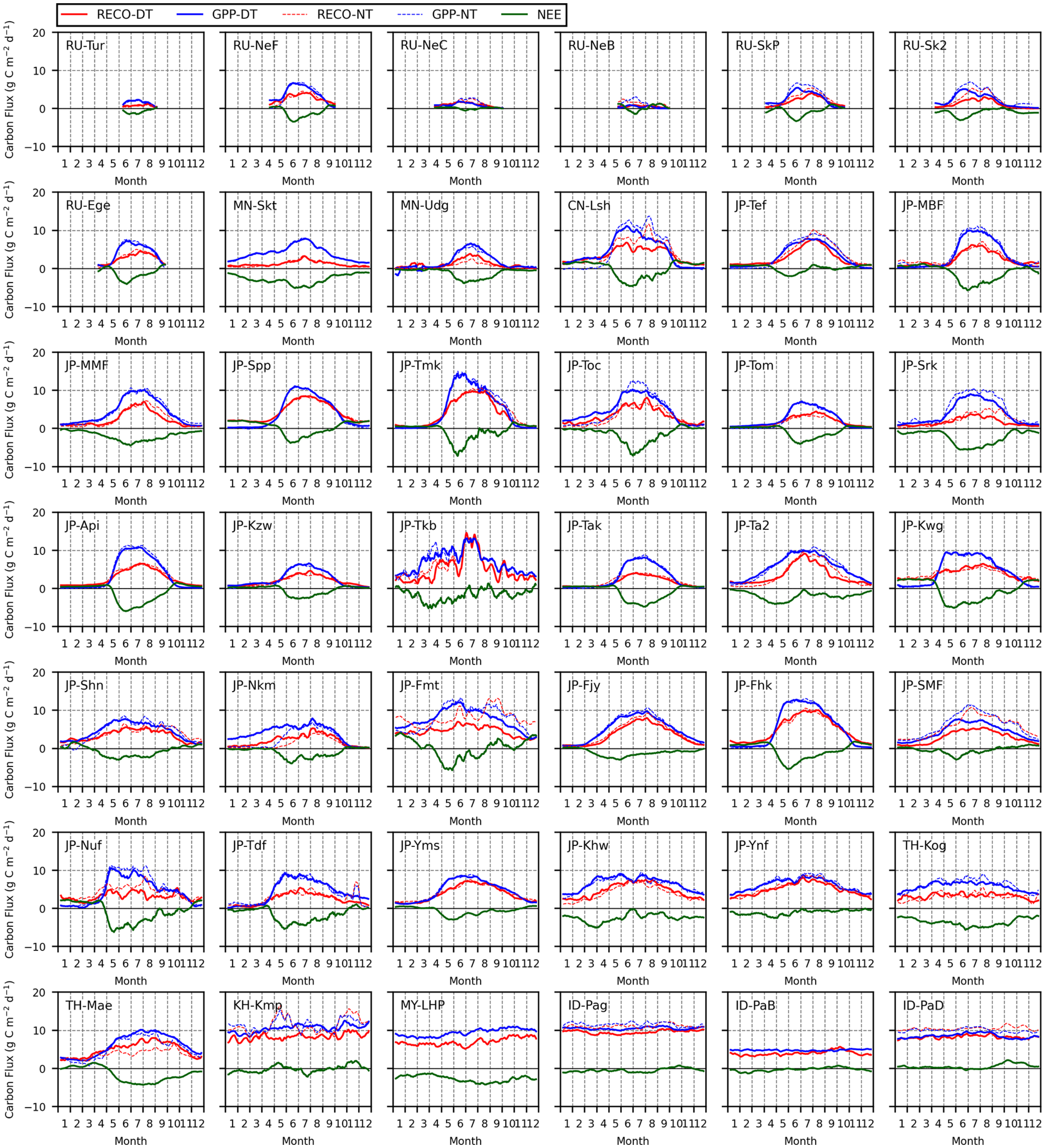

Figure 5. Mean seasonality of GPP, RECO, and NEE across forest sites. GPP and RECO were partitioned using the daytime method (DT, solid lines) or the nighttime method (NT, dashed lines). The seasonality is shown when NEE was measured, and those for GPP and RECO are shown when the partitioning was successful. The seasonality is the ensemble mean of the daily fluxes for each day of the year for all years. The sites are ordered according to latitude from high to low. The mean seasonality is shown for sites having data for at least one growing season.

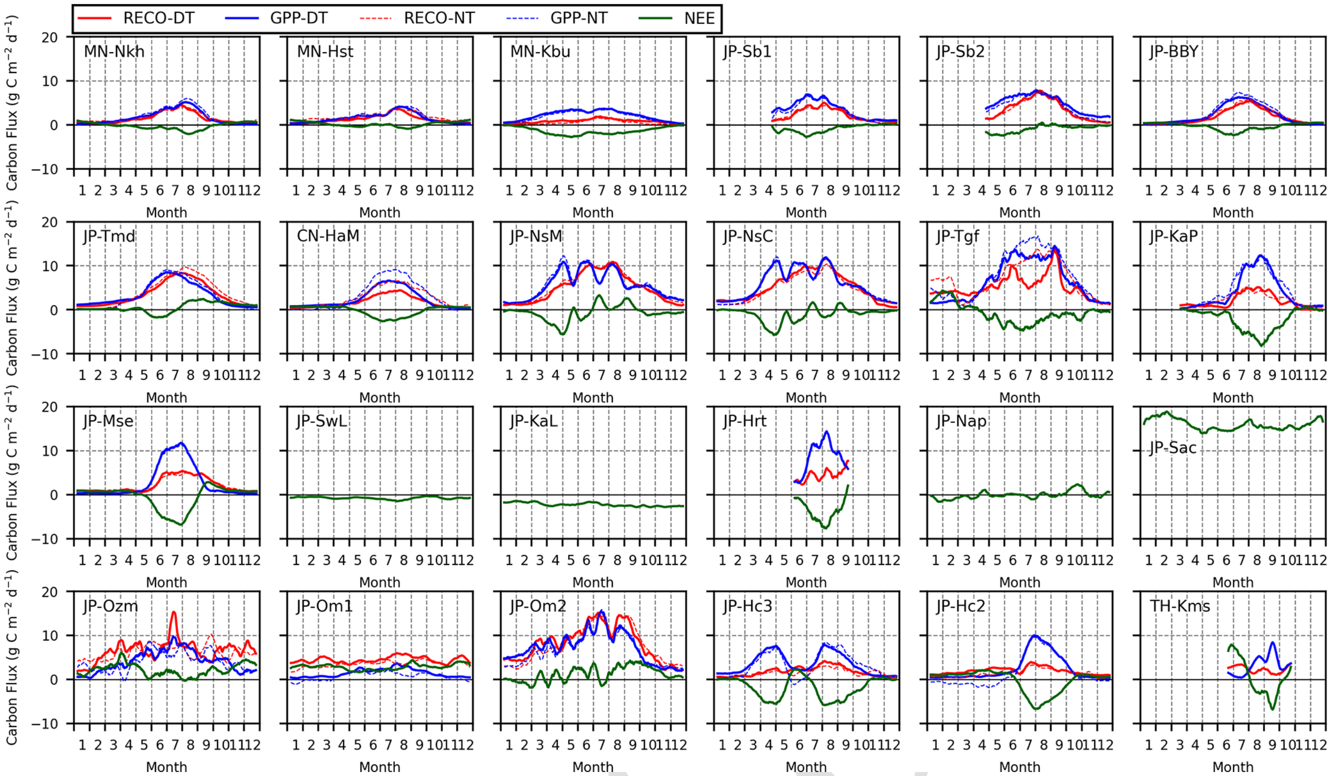

Figure 6. Mean seasonality of GPP, RECO, and NEE across sites other than forests. Designations are as in Fig. 5.

PPFD, and u^*, non-gap-filled data for these variables were included. Gap-filled soil temperature and soil water content were measured at the shallowest depth, while CO_2 concentration was gap-filled for the highest altitude. A quality information flag was assigned for gap-filled variables, where 0 is the original data, 1 is a gap-filled value of the most reliable quality (calculated using a 14 d window), 2 is a gap-filled value of medium quality (calculated using a 14 to 56 d window), and 3 is the gap-filled value of the least reliable quality (calculated using a window longer than 56 d) (Wutzler et al., 2018). If gap-filled CH_4 flux data were provided by the site team (i.e., at JP-BBY), they were included in COREVARS. The COREVARS file was provided with five temporal resolutions (half-hourly/hourly, daily, weekly, monthly, and annual aggregations).

The ALLVARS file included the original, unprocessed data, internal variables (aggregated meteorological variables measured at different locations or with different sensors), and meteorological data from ERA5, in addition to the processed variables included in COREVARS. The ALLVARS file is provided with the five temporal resolutions listed above.

For NEE, GPP, and RECO, the unit was μmol m^{-2} s^{-1} for the half-hourly and hourly timescales; g C m^{-2} d^{-1} for the daily, weekly, and monthly timescales; and g C m^{-2} yr^{-1} for the annual timescale. For CH_4 flux, the unit for the half-hourly and hourly timescales was nmol m^{-2} s^{-1}, whereas the units for the other timescales were the same as those for CO_2 fluxes. The units of precipitation were mm for the half-hourly and hourly timescales; mm d^{-1} for the daily, weekly, and monthly timescales; and mm yr^{-1} for the annual timescale. The units of other variables followed the FLUXNET format (https://ameriflux.lbl.gov/data/aboutdata/data-variables/, last access: 27 December 2024), which did not change with the timescale.

The ERA5 file contains the data for air temperature (TA_ERA5; °C), relative humidity (RH_ERA5; %), VPD (VPD_ERA5; hPa), vapor pressure (e_ERA5; hPa), saturation vapor pressure (e_sat_ERA5; hPa), wind speed (WS_ERA5; m s^{-1}), atmospheric pressure (PA_ERA5; kPa), incoming shortwave radiation (SW_ERA5; W m^{-2}), incoming longwave radiation (LW_ERA5; W m^{-2}), and precipitation (P_ERA5; mm). The ERA5 file is provided with the five temporal resolutions listed above. The variables in the ERA5 file were not corrected for the bias in comparison to the site data.

Two auxiliary files – for meteorology and the u^* threshold – are provided. The AUXMETEO file includes the following statistics for downscaling ERA5 to the site scale: the linear slope between the measured data and ERA5 (ERA_SLOPE), intercept (ERA_INTERCEPT), root mean square error (ERA_RMSE), and correlation coefficient (ERA_CORRELATION). These statistics are included for each year and for all years when measurements were conducted. The TIMESTAMP column in the AUXMETEO file

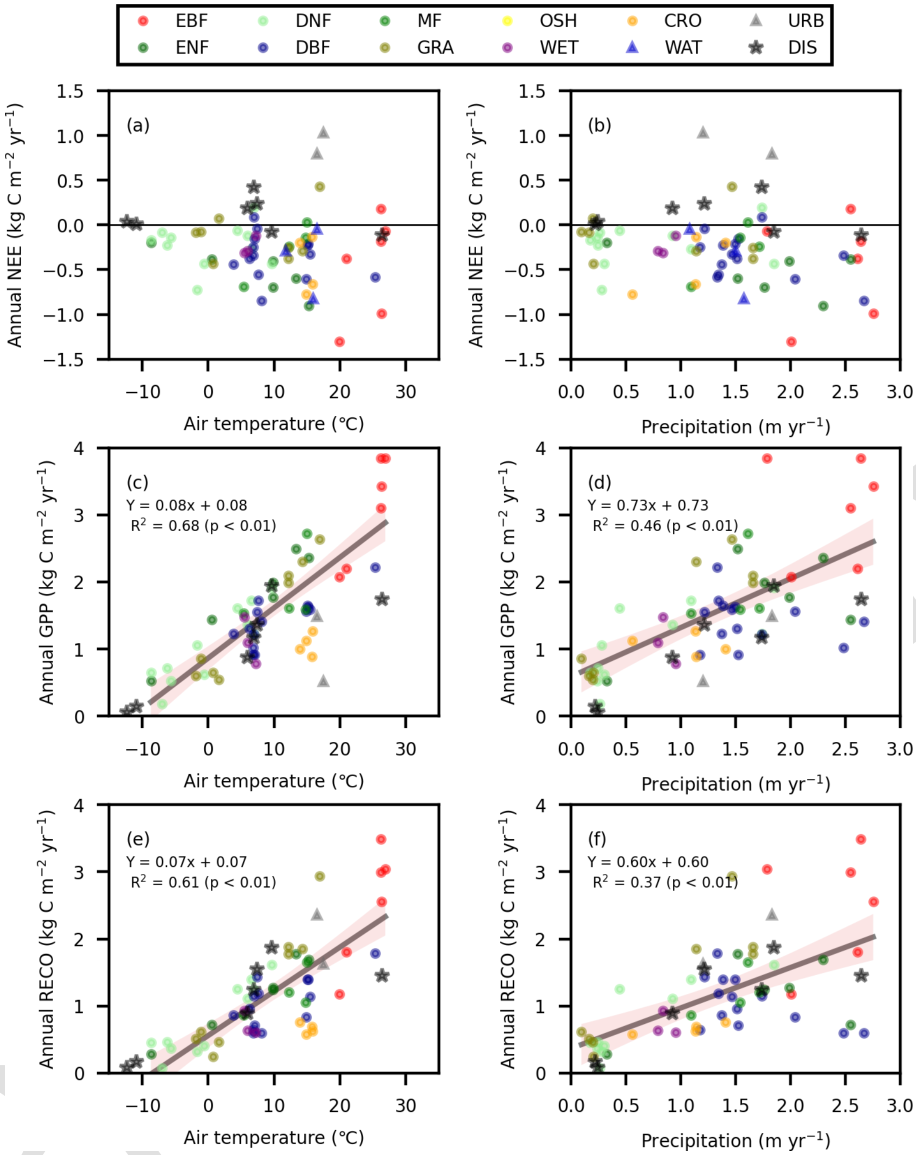

Figure 7. Relationships of annual NEE **(a, b)**, GPP **(c, d)**, and RECO **(e, f)** to the mean climate of the annual mean air temperature **(a, c, e)** and annual sum of the precipitation **(b, d, f)**. GPP and RECO were estimated using the daytime method. The stars represent fluxes obtained at disturbed forests, defined as forests that experienced disturbance within the last 10 years. The annual fluxes were calculated based on the sum of the mean seasonality shown in Figs. 5 and 6; missing measurements during the winter at high latitudes were gap-filled as 0. Because the JP-Spp, JP-Tmd, and JP-Tef sites experienced significant disturbance (windthrow or clearcut) during the measurement period, data obtained within 10 years after a disturbance were classified as disturbed forests (DIS). The lines represent linear regressions, with shading showing the confidence intervals ($p < 0.05$), determined by excluding the DIS data. The annual CO_2 flux for JP-Sac ($5.8\,\mathrm{kg\,C\,m^{-2}\,yr^{-1}}$) is not shown due to the totally different carbon budget in the urban center compared to those in ecosystems. The values are shown in Table 3. Land cover type abbreviations are in Fig. 3.

represents the year for the statistics, where −9999 represents the statistics for the entire year. The AUXNEE file includes the u^* threshold for each year, with the reference threshold and the 5th, 50th, and 95th percentiles of the estimated u^* threshold.

The dataset also includes the BADM files, which are used in the FLUXNET community. Six BADM files are provided: (1) general information, (2) instrument, (3) instrument operations, (4) vegetation cover, (5) soil, and (6) disturbance and management.

Table 3. Summary of mean annual air temperature (TA), annual sum of precipitation (PREC), mean annual downward shortwave radiation (Rsd), mean annual carbon fluxes (NEE, GPP, RECO), mean annual latent heat flux (LE), mean annual sensible heat flux (H), evapotranspiration (ET), and land cover. The statistics were calculated for the observation years; for disturbed sites, the data were considered separately for the periods before, during, and after disturbance. Disturbed ecosystems were defined as those that experienced disturbance within the last 10 years. GPP, RECO, NEE, LE, and ET for boreal forests in Russia that lacked winter measurements (RU-Tur, RU-NeB, RU-NeC, RU-NeF, RU-SkP, RU-Ege, RU-Sk2) were considered 0. GPP, RECO, and NEE at MN-Skt and MN-Kbu were also considered 0 during winter, when the daily mean air temperature was below −5 °C (indicated by asterisks in the table), to mitigate the influence of the negative values of CO_2 fluxes caused by an artifact associated with an open-path sensor. The NA values were listed because missing observations, even after gap-filling fluxes, prevented the calculation of annual fluxes or because the standard flux partitioning was not available for the pond, lakes, and urban landscapes.

Site ID	Disturbance	Land cover	TA	PREC	Rsd	NEE	GPP	RECO	LE	H	ET
			°C	$mm\,yr^{-1}$	$W\,m^{-2}$	$g\,C\,m^{-2}\,yr^{-1}$	$g\,C\,m^{-2}\,yr^{-1}$	$g\,C\,m^{-2}\,yr^{-1}$	$W\,m^{-2}$	$W\,m^{-2}$	$mm\,yr^{-1}$
RU-Tur		DNF	−7.0	264	93	−83	180	76	NA	NA	NA
RU-NeB	fire	GRA	−12.3	244	117	37	57	85	NA	NA	NA
RU-NeF		OSH	−8.6	175	117	−166	653	455	10	NA	132
RU-NeC	clearcut	DIS	−10.9	224	112	12	147	170	13	NA	162
RU-SkP		DNF	−5.7	238	118	−139	523	375	21	NA	265
RU-Sk2		ENF	−8.7	328	117	−194	522	283	16	NA	203
RU-USk		GRA	−11.6	289	110	NA	NA	NA	15	NA	193
RU-Ege		DNF	−6.3	248	122	−225	715	466	20	NA	259
MN-Skt		DNF	−1.7	279	169	−722*	1058*	324*	15	45	189
MN-Udg		DNF	−0.6	303	157	−431	617	413	19	29	246
MN-Nkh		GRA	−1.9	163	171	−83	603	516	20	25	253
MN-Hst		GRA	1.6	197	181	76	541	468	18	27	228
MN-Kbu		GRA	0.7	204	183	−433	647*	248*	9*	30	116
CN-Lsh		DNF	4.4	443	144	−60	1606	1255	25	36	324
JP-Sb1		WET	6.0	794	145	−288	1098	638	NA	NA	NA
JP-Sb2		WET	5.5	840	140	−313	1476	935	NA	NA	NA
JP-Tef	before	DIS	5.9	926	125	192	882	898	18	10	232
	clearcut	GRA	5.9	926	125	−118	1363	1114	27	13	343
	after	MIX	5.9	926	125	−26	1238	1034	21	17	268
JP-MBF		DBF	3.9	1373	134	−442	1233	862	37	20	472
JP-MMF		MF	5.4	1092	134	−689	1537	861	43	21	537
JP-BBY		WET	7.2	953	143	−118	785	610	41	12	524
JP-Spp	before	DIS	7.4	1215	145	235	1366	1554	35	16	444
	windthrow	DBF	7.4	1215	145	−42	1557	1432	40	15	500
JP-Tmk		DNF	6.6	1092	133	−270	1727	1401	45	31	568
JP-Tmd	windthrow	GRA	7.0	1738	139	421	1176	1249	NA	NA	NA
	after	DBF	7.0	1738	139	89	1225	1147	34	21	427
JP-Toc		DBF	7.6	1342	137	−556	1729	1189	33	30	418
JP-Tom		DBF	6.9	1173	128	−249	916	642	NA	40	NA
JP-Srk		DBF	8.1	2669	129	−847	1408	600	41	−1	509
JP-Api		DBF	6.3	1509	150	−375	1307	958	18	14	235
CN-HaM		GRA	−1.1	97	200	−77	862	618	31	23	389
JP-NsM		GRA	12.2	1658	150	−251	1989	1779	55	6	704
JP-NsC		GRA	12.2	1658	150	−376	2098	1880	53	7	674
JP-Kzw		DBF	7.0	1524	165	−155	919	709	15	32	187
JP-Tkb		ENF	13.3	1514	159	−599	2490	1781	45	−7	579
JP-Tak		DBF	6.8	2483	146	−342	1024	597	11	26	135
JP-Ta2		ENF	9.8	1760	148	−695	1990	1247	43	16	546
JP-Tgf		GRA	14.3	1141	153	−291	2307	1851	53	19	681
JP-KaP		CRO	14.9	561	155	−774	1127	584	70	7	894
JP-Mse		CRO	13.9	1407	154	−197	1004	763	67	6	858
JP-SwL		WAT	11.8	1499	178	−287	NA	NA	80	18	1021
JP-KaL		WAT	16.0	1575	163	−826	NA	NA	59	21	759
JP-Kwg		DBF	15.2	1492	151	−214	1631	1393	NA	18	NA
JP-Shn		MF	12.3	1713	167	−242	1612	1211	53	43	675
JP-Nkm		ENF	0.5	2544	162	−381	1442	725	36	−3	445
JP-Fmt		MF	15.0	1611	158	35	2720	1652	71	35	913
JP-Kgu	urbanization	URB	16.5	1400	149	NA	NA	NA	27	41	344
JP-Fjy		ENF	9.9	1989	165	−404	1772	1270	39	20	501
JP-Fhk	before	DIS	9.6	1846	168	−74	1945	1873	43	43	554
	thinning	DNF	9.6	1846	168	−433	1914	1619	40	40	510
JP-SMF		MF	14.8	1543	165	−142	1587	1059	51	23	658
JP-Nuf		DBF	15.4	1465	156	−327	1590	1139	22	16	277

Table 3. Continued.

Site ID	Disturbance	Land cover	TA	PREC	Rsd	NEE	GPP	RECO	*LE*	*H*	ET
			°C	$mm\,yr^{-1}$	$W\,m^{-2}$	$g\,C\,m^{-2}\,yr^{-1}$	$g\,C\,m^{-2}\,yr^{-1}$	$g\,C\,m^{-2}\,yr^{-1}$	$W\,m^{-2}$	$W\,m^{-2}$	$mm\,yr^{-1}$
JP-Tdf		DBF	14.8	2039	155	−601	1559	840	45	19	584
JP-Yms		DBF	15.0	1384	159	−223	1644	1400	63	30	805
JP-Nap		WAT	16.5	1083	176	−48	NA	NA	60	9	773
JP-Ako		EBF	15.3	739	169	NA	NA	NA	27	47	347
JP-Sac	urbanization	URB	16.4	1594	159	5807	NA	NA	28	43	354
JP-Ozm	urbanization	URB	16.5	1828	150	793	1485	2353	52	23	673
JP-Om1	urbanization	URB	17.5	1202	165	1032	515	1622	23	39	294
JP-Om2	mowing	GRA	16.9	1466	166	430	2634	2937	71	9	908
JP-Hc3		CRO	15.8	1136	175	−663	1265	625	51	10	659
JP-Hc2		CRO	15.7	1141	161	−132	890	697	60	10	772
JP-Khw		ENF	15.2	2294	158	−906	2359	1689	81	20	1044
JP-Ynf		EBF	20.9	2611	159	−374	2200	1808	65	5	834
TH-Kog		EBF	19.9	2004	183	−1301	2078	1178	73	23	935
TH-Mae		DBF	25.3	1333	205	−579	2215	1783	69	36	888
KH-Kmp		EBF	26.9	1786	206	−72	3842	3044	106	19	1368
MY-LHP		EBF	26.2	2752	184	−989	3431	2552	89	28	1157
ID-Pag		EBF	26.1	2639	200	−183	3840	3486	111	29	1430
ID-PaB	fire	OSH	26.4	2642	197	−110	1746	1450	90	27	1164
ID-PaD		EBF	26.2	2543	197	179	3100	2997	94	29	1215

3 Database summary

3.1 CO_2 flux

Based on the dataset constructed, mean seasonalities in NEE, GPP, and RECO were as expected from the biomes and mean climatology (Figs. 5, 6). In northern boreal forests in Siberia (RU-Tur, RU-NeF, RU-SkP, RU-Sk2), the magnitude of the flux was generally low, and growing seasons when GPP was not negligible were short. In the southern Eurasian boreal forests in Siberia and Mongolia (RU-Ege, MN-Udg, MN-Skt), the magnitudes of CO_2 fluxes were greater than those in the above northern boreal forests. Inland grasslands in Mongolia (MN-Nkh, MN-Hst, MN-Kbu) had smaller CO_2 flux magnitudes than the nearby forests (MN-Udg, MN-Skt). For temperate forest and grassland sites, the dataset showed known seasonality with spring onset, summer peak, and autumn senescence, with low fluxes in winter. Among forest sites, seasonal variations became smaller in the subtropics (JP-Ynf), and clear seasonality disappeared in the tropics (KH-Kmp, MY-LHP, ID, Pag, ID-PaD, ID-PaB) as the climate became warmer. Among rice paddies, single-cropping sites had a single peak (JP-Mse, JP-Hc2), but a double cropping site had two peaks (JP-Hc3) in GPP, RECO, and NEE (Fig. 6). For lakes (JP-SwL, JP-KaL), a pond (JP-Nap), and an urban center (JP-Sac), CO_2 fluxes showed smaller seasonality than those at vegetation surfaces.

Some data for CO_2 fluxes raise suspicions. First, markedly negative NEE values in harsh winters were estimated for MN-Skt and MN-Kbu (Figs. 5, 6), which could be caused by an artifact known for the open path sensor (Burba et al., 2008). The artificially negative NEE caused a considerable positive GPP in winter. Data users should be cautious about the data for MN-Skt and MN-Kbu. Second, the daytime partitioning method extrapolated the relationship obtained during the growing season to winters when NEE was not measured. The result was erroneous estimation of GPP and RECO (e.g., JP-Nkm in Fig. 5). Using the nighttime approach, GPP and RECO were not estimated for the period when NEE was not measured. Despite these suspicious data, the fluxes partitioned using the nighttime and daytime methods were generally consistent across the sites.

The spatial variabilities in annual NEE, GPP, and RECO were also consistent with earlier reports for Asian ecosystems (Fig. 7; Table 3). In Asia, the spatial variabilities in GPP and RECO are explained mostly by the mean annual air temperature (Hirata et al., 2008; Kato and Tang, 2008; Saigusa et al., 2013; Yu et al., 2013). Except in disturbed forests and croplands, GPP and RECO increased linearly with mean annual air temperature (Fig. 7). Correlations of GPP and RECO with the annual sum of precipitation were lower than with the mean annual air temperature. No clear correlation was found between annual NEE and mean annual air temperature or annual sum of precipitation, but the maximum CO_2 sink (i.e., negative NEE) with each temperature range appeared to be increased by temperature up to the annual mean temperature range until approximately 10 °C (Fig. 7a). Except for disturbed forests and urban sites, most ecosystems were estimated to be a CO_2 sink of up to $1.0\,kg\,C\,m^{-2}\,yr^{-1}$.

In the developed dataset, annual CO_2 fluxes tended to differ by land cover type (Fig. 8). Forest ecosystems included in the datasets had, on average, similar CO_2 sinks. Among the forest ecosystems, the mean CO_2 sink tended to be highest in ENF. GPP and RECO in temperate managed grasslands were higher than those in natural grasslands in Mongolia and Russia. The annual CO_2 sink also tended to be greater in managed grasslands compared to natural grasslands, except for

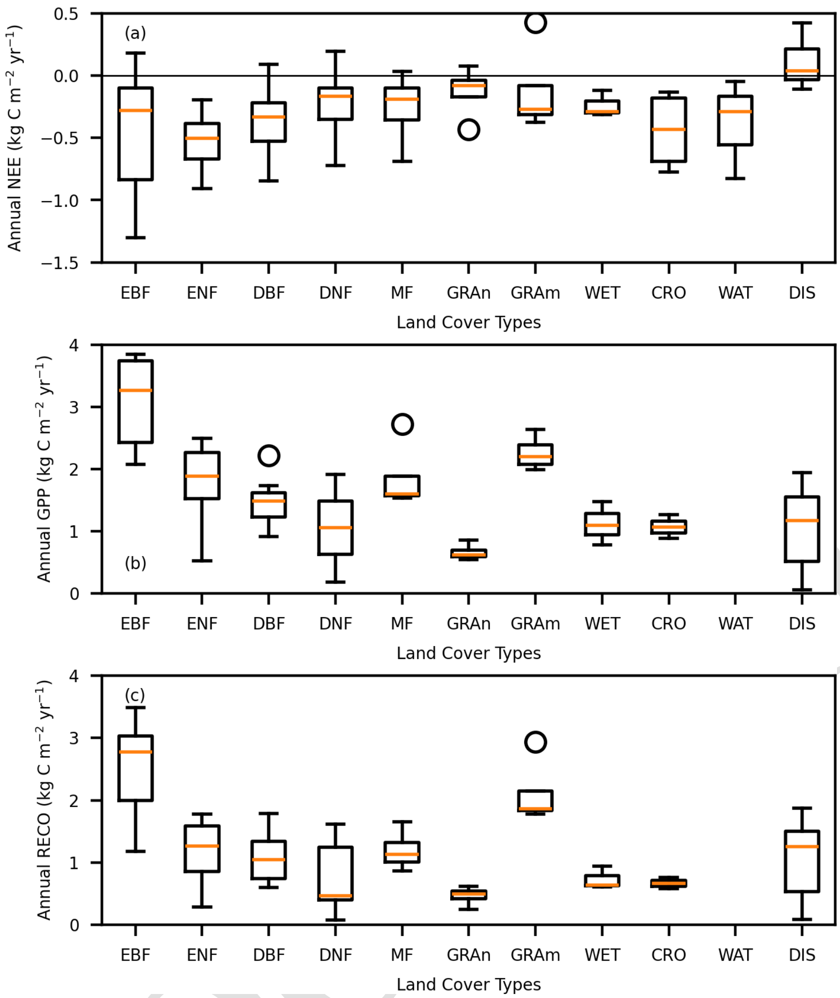

Figure 8. Boxplots for annual NEE, GPP, and RECO by land cover type. GPP and RECO were estimated using the daytime method. Fluxes at urban sites are not shown because the range of urban CO_2 emissions was totally different from those for vegetation or lakes. Because flux partitioning was not conducted for lakes and ponds, partitioned fluxes for these water surfaces were not shown. Land cover type abbreviations are in Fig. 3, although the grassland category was separated into natural grassland (GRAn) and managed grassland (GRAm). The definition of DIS was the same as in Fig. 7, where all data from RU-NeC, RU-NeB, and ID-PaB are also classified as DIS. The box represents the interquartile range (25th to 75th percentiles), the whiskers represent the maximum and minimum values, excluding outliers shown by circles, and the orange bar represents the median value.

a frequently mowed site (JP-Om2), which exhibited net annual CO_2 emissions. Disturbed forests, on average, acted as a small CO_2 source. CO_2 emissions in urban centers (JP-Sac; 5.8 kg C m^{-2} yr^{-1}; not included in Fig. 8a) were considerably higher than those from natural or agricultural ecosystems. The annual GPP was highest in EBF among forest ecosystems, followed by ENF, DBF, and DNF. RECO was highest in EBF, whereas those in ENF, DBF, and DNF were similar to each other. Annual GPP and RECO varied greatly among grasslands because they included inland dry grasslands and Japan's weedy grasslands (Fig. 8b, c).

3.2 Energy fluxes

Mean annual energy fluxes represented in the dataset were explained better by air temperature than precipitation (Fig. 9; Table 3). The mean annual LE increased with the mean annual air temperature; their strong linear correlation could be explained by a close coupling between transpiration and photosynthesis (Medlyn et al., 2011), where spatial variations in annual GPP were strongly correlated with annual air temperature (Fig. 7c). Evaporation could also be enhanced under high air temperature and resulting high VPD conditions (Zhang et al., 2016). The dataset included mostly ecosystems around the Pacific Ocean, which were especially densely distributed in Japan, whereas water-limited inland ecosystems were scarce. Consequently, the correlation between LE and

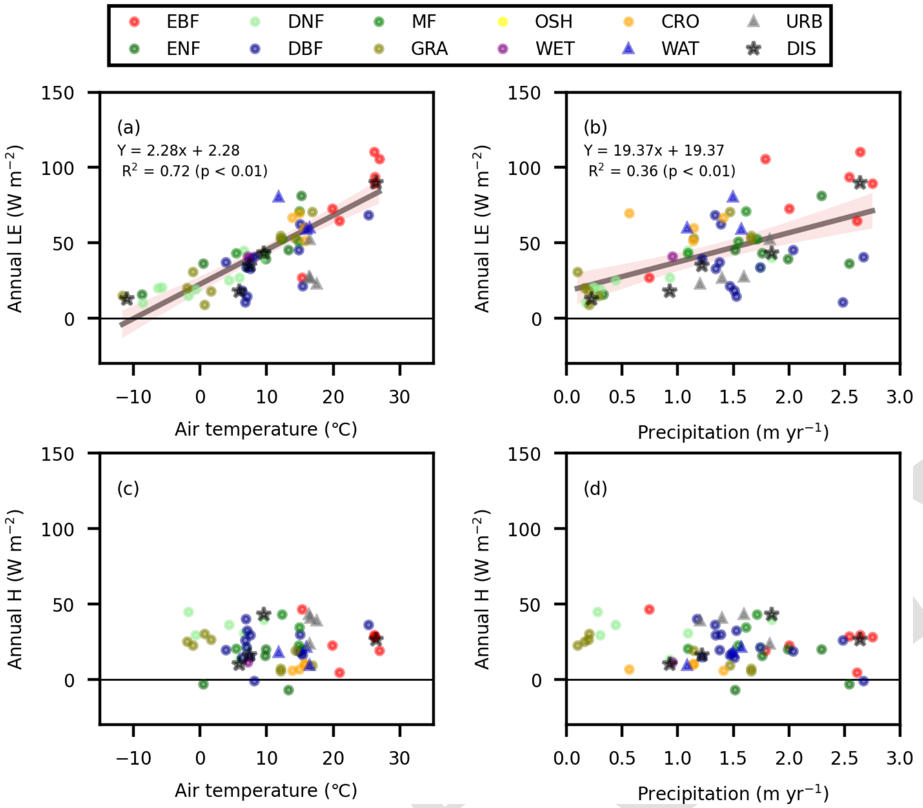

Figure 9. Relationships of annual energy fluxes of the latent heat flux (LE) **(a, b)** and sensible heat flux (H) **(c, d)** to the mean climate of the annual mean air temperature **(a, c)** and annual sum of the precipitation **(b, d)**. The classification of the disturbed forest (DIS) is as in Fig. 8. Annual H values were calculated only for the case where there were no missing data in the mean seasonality, whereas the missing LE data during the winter were considered to be 0 for boreal forests in Russia. The lines represent linear regressions, with shading showing the confidence intervals ($p < 0.05$), determined by excluding the data from DIS, urban areas (URB), and lakes and ponds (WAT). The values are shown in Table 3. Land cover type abbreviations are in Fig. 3.

precipitation was weaker than those reported in a literature survey for Asia (Kang and Cho, 2021). Under similar climate conditions, LE was lower and H was higher in urban landscapes compared with vegetation surfaces, in agreement with a previous report (Ueyama et al., 2021). Mean annual H did not change with air temperature or precipitation, possibly caused by missing high-latitude observations owing to missing winter data (e.g., RU-Tur, RU-SkP, RU-Ege) (Fig. 5). Negative H values in high-latitude ecosystems were observed owing to decreased available energy associated with the snow albedo (Nakai et al., 2013; Ueyama et al., 2020b).

4 Data availability

The dataset associated with this publication can be found at the ADS website (https://ads.nipr.ac.jp/japan-flux2024/TS4), where individual site data have their own DOIs. All data are available under the CC BY 4.0 copyright policy with appropriate citations of this paper. We suggest that researchers planning to use this dataset as a core dataset for their analysis contact and collaborate with database developers and relevant site teams. As in the data policy of FLUXNET2015, in case of a synthesis using both CC BY 4.0 and other private data, all data should be treated as Tier Two of the FLUXNET data policy (data producers must have opportunities to collaborate and consult with data users).

5 Conclusions

The JapanFlux2024 dataset is the first public dataset that includes as much data as possible, both old and new, as an activity of JapanFlux. The dataset is consistent with previous synthesis studies in Asia in terms of seasonalities in CO_2 and energy fluxes across Japan and East Asia but substantially increased the amount of data, i.e., 83 sites with 683 site-years from 1990 to 2023. The dataset will facilitate important studies in East Asia, including Japan, such as those on land–atmosphere interactions, improvement of process models, and upscaling fluxes using machine learning. Because the dataset is processed in line with selected procedures from the FLUXNET standard dataset, the JapanFlux2024 dataset will bridge collaborations between researchers from Asia and FLUXNET.

Author contributions. The JapanFlux2024 dataset was conceptualized by MU. The standardized dataset was prepared by MU and YT, and the metadata was compiled by HY and TH in collaboration with the data contributors. The data distribution website was developed by a team led by HY. KI contributed to the editing of the paper. The remaining co-authors contributed eddy covariance data to the dataset and/or participated in the editing of the paper.

Competing interests. The contact author has declared that none of the authors has any competing interests.

Disclaimer. Publisher's note: Copernicus Publications remains neutral with regard to jurisdictional claims made in the text, published maps, institutional affiliations, or any other geographical representation in this paper. While Copernicus Publications makes every effort to include appropriate place names, the final responsibility lies with the authors.

Acknowledgements. The development of the database was supported by the digital biosphere project under KAKENHI (21H05316, to Tomo'omi Kumagai), PAWCs project under KAKENHI (19H05668), JSPS A3 Foresight Program (JPJSA3F20220002), and Arctic Challenge for Sustainability II (ArCS II; JPMXD1420318865). The CH-Lsh data were provided by Nobuko Saigusa of the National Institute of Environmental Studies and Huimin Wang of the Chinese Academy of Sciences. Observations at JP-Tmk were supported by Ryuichi Hirata of the National Institute of Environmental Studies. Observations of JP-Kgu were supported by Manabu Kanda of the Institute of Science Tokyo. Observations of JP-Tdf were supported by Shigeaki Hattori of Nagoya University. Observations of JP-Ynf were supported by Shingo Tanigushi of the University of the Ryukyus. Masahito Ueyama was supported by KAKENHI (18H03362, 24K03065). Sachinobu Ishida was supported by KAKENHI (25450201). Kazuhito Ichii, Hiromi Yazawa, and Makiko Tanaka were supported by KAKENHI (22H05711, 22H05004, 24H01504) and the Environment Research and Technology Development Fund (JPMEERF24S12207). Hiroki Iwata was supported by KAKENHI (17H05039, 21H02315, 23K21248, 23KK0194). Michiaki Sugita was supported by KAKENHI (15K01159, 20H01384, 23K20125). Takanori Shimizu was supported by KAKENHI (20H0309). Multidisciplinary observations at Takayama sites (JP-Tak and JP-Ta2) were supported jointly by Hiroyuki Muraoka (KAKENHI 21H05316, 21H05312, 19H03301), Taku M. Saitoh (KAKENHI 18780113, 21241009, 22248017, 23710005, 24241008, 26241005, 26292092, 15H04512, 20H03041, 20K06144, 21H02245, 21H05316, 23K11395, 24K01818, 24K00986, the Environment Research and Technology Development Fund (JPMEERF20232M01) of the Environmental Restoration and Conservation Agency provided by the Ministry of the Environment of Japan, the Global Environment Research Coordination System from the Ministry of the Environment, Japan MAFF2254), Hiroaki Kondo, Shohei Murayama, Shigeyuki Ishidoya, and Takahisa Maeda (KAKENHI 24241008, 24310017, 15H02814, 18H03365, 19H01975, 22H00564, 22H05006, Global Environment Research Coordination System from the Ministry of the Environment, Japan MAFF0751, MAFF1251, MAFF2254, the Global Environment Research Fund of the Ministry of the Environment, Japan S-1: Integrated Study for Terrestrial Carbon Management of Asia in the 21st Century Based on Scientific Advancement). JP-Spp, JP-Api, JP-Fjy, JP-Yms, and JP-Khw were supported by KAKEN (16K07789), Research revolution 2002: Global Warming Initiatives (FY2002-2006) by the Ministry of Education, Culture, Sports, Science, and Technology of Japan, Commissioned project study from the Ministry of Agriculture, Forestry, and Fisheries (JPJ005317), Environment Research and Technology Development Fund (S-1), and Research Coordination System (MAFF0751, 1251, 2254) from the Ministry of the Environment of Japan, and research grants (#199903, #200303, #201802) from the Forestry and Forest Products Research Institute. JP-Tom was supported by KAKENHI (11213204, 14656059, 16208014, 2331001513, 2529207903) and by the Ministry of the Environment (0708BD437, D-0909), given to Tsutom Hiura. JP-Mse was supported by the Global Environmental Research Fund (S-1) of the Ministry of Environment of Japan, a research project entitled "Development of technologies for mitigation and adaptation to climate change in agriculture, forestry, and fisheries" by the Ministry of Agriculture, Forestry, and Fisheries of Japan, and KAKENHI (19H03077, 19H03085, 23H02341). Kazuho Matsumoto was supported by KAKENHI (25304027, 16H02762, 21H02238, 22K05752, 24H01520). Trofim Maximov was partly supported by the project "Study of biogeochemical cycles and adaptive reactions of plants of boreal and arctic ecosystems of northeastern Russia" (AAAA-A21-121012190034-2) of the Ministry of Education and Science of Russia. We thank the two anonymous reviewers and Dario Papale for their constructive comments and suggestions.

Financial support. This research has been supported by the Japan Society for the Promotion of Science (grant nos. 21H05316, 19H05668, and JPJSA3F20220002) and the Ministry of Education, Culture, Sports, Science, and Technology (grant no. JPMXD1420318865). TS5

Review statement. This paper was edited by Hanqin Tian and reviewed by Dario Papale and two anonymous referees.

References

Asanuma, J.: JapanFlux2024 MN-Kbu Kherlenbayan Ulaan, 1.00, Arctic Data archive System (ADS) [data set], https://doi.org/10.17592/001.2024121004, 2025a.

Asanuma, J.: JapanFlux2024 MN-Skt Southern Khentei Taiga, 1.00, Arctic Data archive System (ADS) [data set], https://doi.org/10.17592/001.2024121011, 2025b.

Asanuma, J. and Shimoda, S.: JapanFlux2024 JP-Tgf Terrestrial Environment Research Center, University of

Tsukuba, 1.00, Arctic Data archive System (ADS) [data set], https://doi.org/10.17592/001.2024121013, 2025.

Awal, M. A. and Ohta, T.: JapanFlux2024 JP-Nuf Nagoya University Forest, 1.00, Arctic Data archive System (ADS) [data set], https://doi.org/10.17592/001.2024121008, 2025a.

Awal, M. A. and Ohta, T.: JapanFlux2024 JP-Tdf Toyota Deciduous Forest, 1.00, Arctic Data archive System (ADS) [data set], https://doi.org/10.17592/001.2024121012, 2025b.

Awal, M. A., Ohta, T., Matsumoto, K., Toba, T., Daikoku, K., Hattori, S., Hiyama, T., and Park, H.: Comparing the carbon sequestration capacity of temperate deciduous forests between urban and rural landscapes in central Japan, Urban For. Urban Gree., 9, 261–170, https://doi.org/10.1016/j.ufug.2010.01.007, 2010.

Baldocchi, D., Novick, K., Keenan, T., and Torn, M.: AmeriFlux: Its Impact on our understanding of the “breathing of the biosphere”, after 25 years, Agr. Forest Meteorol., 348, 109929, https://doi.org/10.1016/j.agrformet.2024.109929, 2024.

Beer, C., Reichstein, M.,Tomelleri, E., Ciais, P., Jung, M., Carvalhais, N., Rödenbeck, C., Arain, M. A., Baldocchi, D., Bonan, G. B., Bondeau, A., Cescatti, A., Lasslop, G., Lindroth, A., Lomas, M., Luyssaert, S., Margolis, H., Oleson, K. W., Roupsard, O., Veenendaal, E., Viovy, N., Williams, C., Ian Woodward, F., and Papale, D.: Terrestrial Gross Carbon Dioxide Uptake: Global Distribution and Covariation with Climate, Science, 329, 834–838, https://doi.org/10.1126/science.1184984, 2010.

Boiarskii, B. and Hasegawa, H.: Comparison of NDVI and NDRE Indices to Detect Differences in Vegetation and Chlorophyll Content, Internatl. Conf. Appl. Sci., Tech. Engin. J. Mech. Cont. & Math. Sci., 4, 20–29, https://doi.org/10.26782/jmcms.spl.4/2019.11.00003, 2019.

Bonan, G. B., Oleson, K. W., Fisher, R. A., Lasslop, G., and Reichstein, M.: Reconciling leaf physiological traits and canopy flux data: Use of the TRY and FLUXNET databases in the Community Land Model version 4, J. Geophys. Res.-Biogeo., 117, G02026, https://doi.org/10.1029/2011JG001913, 2012.

Bond-Lamberty, B., Christianson, D. S., Malhotra, A., Pennington, S. C., Sihi, D., Agha-Kouchak, A., Anjileli, H., Arain, M. A., Armesto, J. J., Ashraf, S., Ataka, M,, Baldocchi, D., Black, T. A., Buchmann, N., Carbone, M. S., Chang, S.-C., Crill, P., Curtis, P. S., Davidson, E. A., Desai, A. R., Drake, J., El-Madany, T. S., Gavazzi, M., Görres, C.-M., Gough, C. M., Goulden, M., Gregg, J., del Arroyo, O. G., He, J.-S., Hirano, T., Hopple, A., Hughes, H., Järveoja, J., Jassal, R., Jian, J., Kan, H., Kaye, J., Kominami, Y., Liang, N., Lipson, D., Macdonald, C., Maseyk, K., Mathes, K., Mauritz, M., Mayes, M. A., McNulty, S., Miao, G., Migliavacca, M., Miller, S., Miniat, C. F., Nietz, J. G., Nilsson, M. B., Noormets, A., Norouzi, H., O’Connell, C. S., Osborne, B., Oyonarte, C., Pang, Z., Peichl, M., Pendall, E., Perez-Quezada, J. F., Phillips, C. L., Phillips, R. P., Raich, J. W., Renchon, A. A., Ruehr, N. K., Sánchez-Cañete, E. P., Saunders, M., Savage, K. E., Schrumpf, M., Scott, R. L., Seibt, U., Silver, W. L., Sun, W., Szutu, D., Takagi, K., Takagi, M., Teramoto, M., Tjoelker, M. G., Trumbore, S., Ueyama, M., Vargas, R., Varner, R. K., Verfaillie, J., Vogel, C., Wang, J., Winston, G., Wood, T. E., Wu, J., Wutzler, T., Zeng, J., Zha, T., Zhang, Q., and Zou, J.: COSORE: A community database for continuous soil respiration and other soil-atmosphere greenhouse gas flux data, Glob. Change Biol., 26, 7268–7283, https://doi.org/10.1111/gcb.15353, 2020.

Burba, G., McDermitt, D. K., Grelle, A., Anderson, D. J., and Xu, L.: Addressing the influence of instrument surface heat exchange on the measurements of CO_2 flux from open-path gas analyzers, Glob. Change Biol., 14, 1854–1876, https://doi.org/10.1111/j.1365-2486.2008.01606.x, 2008.

Delwiche, K. B., Knox, S. H., Malhotra, A., Fluet-Chouinard, E., McNicol, G., Feron, S., Ouyang, Z., Papale, D., Trotta, C., Canfora, E., Cheah, Y.-W., Christianson, D., Alberto, Ma. C. R., Alekseychik, P., Aurela, M., Baldocchi, D., Bansal, S., Billesbach, D. P., Bohrer, G., Bracho, R., Buchmann, N., Campbell, D. I., Celis, G., Chen, J., Chen, W., Chu, H., Dalmagro, H. J., Dengel, S., Desai, A. R., Detto, M., Dolman, H., Eichelmann, E., Euskirchen, E., Famulari, D., Fuchs, K., Goeckede, M., Gogo, S., Gondwe, M. J., Goodrich, J. P., Gottschalk, P., Graham, S. L., Heimann, M., Helbig, M., Helfter, C., Hemes, K. S., Hirano, T., Hollinger, D., Hörtnagl, L., Iwata, H., Jacotot, A., Jurasinski, G., Kang, M., Kasak, K., King, J., Klatt, J., Koebsch, F., Krauss, K. W., Lai, D. Y. F., Lohila, A., Mammarella, I., Belelli Marchesini, L., Manca, G., Matthes, J. H., Maximov, T., Merbold, L., Mitra, B., Morin, T. H., Nemitz, E., Nilsson, M. B., Niu, S., Oechel, W. C., Oikawa, P. Y., Ono, K., Peichl, M., Peltola, O., Reba, M. L., Richardson, A. D., Riley, W., Runkle, B. R. K., Ryu, Y., Sachs, T., Sakabe, A., Sanchez, C. R., Schuur, E. A., Schäfer, K. V. R., Sonnentag, O., Sparks, J. P., Stuart-Haëntjens, E., Sturtevant, C., Sullivan, R. C., Szutu, D. J., Thom, J. E., Torn, M. S., Tuittila, E.-S., Turner, J., Ueyama, M., Valach, A. C., Vargas, R., Varlagin, A., Vazquez-Lule, A., Verfaillie, J. G., Vesala, T., Vourlitis, G. L., Ward, E. J., Wille, C., Wohlfahrt, G., Wong, G. X., Zhang, Z., Zona, D., Windham-Myers, L., Poulter, B., and Jackson, R. B.: FLUXNET-CH4: a global, multi-ecosystem dataset and analysis of methane seasonality from freshwater wetlands, Earth Syst. Sci. Data, 13, 3607–3689, https://doi.org/10.5194/essd-13-3607-2021, 2021.

Delwiche, K. B., Nelson, J., Kowalska, N., Moore, C. E., Shirkey, G., Tarin, T., Cleverly, J. R., and Keenan, T. F.: Charting the Future of the FLUXNET Network, B. Am. Meteorol. Soc., 105, E466–E473, https://doi.org/10.1175/BAMS-D-23-0316.1, 2024.

Du, M., Li, Y., Zhang, F., Zhao, L., Li, H., Gu, S., Yonemura, S., and Tang, Y.: Characteristics and scenarios projection of NEE change in an alpine meadow on the Tibetan Plateau, Internatl. J. Glob. Warming, 24, 307–325, https://doi.org/10.1504/IJGW.2021.116711, 2021.

Du, M., Kato, T., Tang, Y., Li, Y., Gu, S., Zhao, L., and Zhang, F.: JapanFlux2024 CN-HaM Qinghai Flux Research Site, 1.00, Arctic Data archive System (ADS) [data set], https://doi.org/10.17592/001.2024102214, 2025.

Falge, E., Baldocchi, D., Olson, R., Anthoni, P., Aubinet, M., Bernhofer, C., Burba, G., Ceulemans, R., Clement, R., Dolman, H., Granier, A., Gross, P., Grünwald, T., Hollinger, D., Jensen, N.-O., Katul, G., Keronen, P., Kowalski, A., Lai, C. T., Law B. E., Meyers, T., Moncrieff, J., Moors, E.. Munger, W., Pilegaard, K., Rannik, Ü., Rebmann, C., Suyker, A., Tenhunen, J., Tu, K., Verma, S., Vesala, T., Wilson, K., and Wofsy, S.: Gap filling strategies for defensible annual sums of net ecosystem exchange, Agr. Forest Meteorol., 107, 43–69, https://doi.org/10.1016/S0168-1923(00)00225-2, 2001.

Friedlingstein, P., O’Sullivan, M., Jones, M. W., Andrew, R. M., Bakker, D. C. E., Hauck, J., Landschützer, P., Le Quéré, C., Luijkx, I. T., Peters, G. P., Peters, W., Pongratz, J., Schwingshackl, C., Sitch, S., Canadell, J. G., Ciais, P., Jackson, R. B., Alin, S. R., Anthoni, P., Barbero, L., Bates, N. R., Becker, M., Bellouin, N., Decharme, B., Bopp, L., Brasika, I. B. M., Cadule, P., Chamberlain, M. A., Chandra, N., Chau, T.-T.-T., Chevallier, F., Chini, L. P., Cronin, M., Dou, X., Enyo, K., Evans, W., Falk, S., Feely, R. A., Feng, L., Ford, D. J., Gasser, T., Ghattas, J., Gkritzalis, T., Grassi, G., Gregor, L., Gruber, N., Gürses, Ö., Harris, I., Hefner, M., Heinke, J., Houghton, R. A., Hurtt, G. C., Iida, Y., Ilyina, T., Jacobson, A. R., Jain, A., Jarníková, T., Jersild, A., Jiang, F., Jin, Z., Joos, F., Kato, E., Keeling, R. F., Kennedy, D., Klein Goldewijk, K., Knauer, J., Korsbakken, J. I., Körtzinger, A., Lan, X., Lefèvre, N., Li, H., Liu, J., Liu, Z., Ma, L., Marland, G., Mayot, N., McGuire, P. C., McKinley, G. A., Meyer, G., Morgan, E. J., Munro, D. R., Nakaoka, S.-I., Niwa, Y., O'Brien, K. M., Olsen, A., Omar, A. M., Ono, T., Paulsen, M., Pierrot, D., Pocock, K., Poulter, B., Powis, C. M., Rehder, G., Resplandy, L., Robertson, E., Rödenbeck, C., Rosan, T. M., Schwinger, J., Séférian, R., Smallman, T. L., Smith, S. M., Sospedra-Alfonso, R., Sun, Q., Sutton, A. J., Sweeney, C., Takao, S., Tans, P. P., Tian, H., Tilbrook, B., Tsujino, H., Tubiello, F., van der Werf, G. R., van Ooijen, E., Wanninkhof, R., Watanabe, M., Wimart-Rousseau, C., Yang, D., Yang, X., Yuan, W., Yue, X., Zaehle, S., Zeng, J., and Zheng, B.: Global Carbon Budget 2023, Earth Syst. Sci. Data, 15, 5301–5369, https://doi.org/10.5194/essd-15-5301-2023, 2023.

Hamada, S., Ohta, T., Hiyama, T., Kuwada, T., Takahashi, A., and Maximov, T. C.: Hydrometeorological behaviour of pine and larch forests in eastern Siberia, Hydrol. Process., 18, 23–29, https://doi.org/10.1002/hyp.1308, 2004.

Hammerle, A., Haslwanter, A., Schmitt, M., Bahn, M., Tappeiner, U., Cernusca, A., and Wohlfahrt, G.: Eddy covariance measurements of carbon dioxide, latent and sensible energy fluxes above a meadow on a mountain slope, Bound.-Lay. Meteorol., 122, 397–416, https://doi.org/10.1007/s10546-006-9109-x, 2007.

Harazono, Y.: JapanFlux2024 JP-Nsb NIAES Soybean, 1.00, Arctic Data archive System (ADS) [data set], https://doi.org/10.17592/001.2024102240, 2025a.

Harazono, Y.: JapanFlux2024 JP-Yrp Yawara Rice paddy, 1.00, Arctic Data archive System (ADS) [data set], https://doi.org/10.17592/001.2024121019, 2025b.

Harazono, Y.: JapanFlux2024 JP-Hc1 Hachihama Experimental Farm: the International Rice Experiment, 1.00, Arctic Data archive System (ADS) [data set], https://doi.org/10.17592/001.2024102237, 2025c.

Harazono, Y. and Miyata, A.: JapanFlux2024 JP-Km1 Kushiro Mire: Onnenai Fen, 1.00, Arctic Data archive System (ADS) [data set], https://doi.org/10.17592/001.2024102239, 2025a.

Harazono, Y. and Miyata, A.: JapanFlux2024 JP-Km2 Kushiro Mire: Akanuma Bog, 1.00, Arctic Data archive System (ADS) [data set], https://doi.org/10.17592/001.2024121026, 2025b.

Harazono, Y. and Takagi, K.: JapanFlux2024 CN-In1 Inner Mongolia dune, 1.00, Arctic Data archive System (ADS) [data set], https://doi.org/10.17592/001.2024102241, 2025a.

Harazono, Y. and Takagi, K.: JapanFlux2024 CN-In2 Inner Mongolia grassland, 1.00, Arctic Data archive System (ADS) [data set], https://doi.org/10.17592/001.2024102242, 2025b.

Harazono, Y. and Takagi, K.: JapanFlux2024 CN-In3 Inner Mongolia soybean, 1.00, Arctic Data archive System (ADS) [data set], https://doi.org/10.17592/001.2024102243, 2025c.

Harazono, Y. and Takagi, K.: JapanFlux2024 CN-In4 Inner Mongolia maize, 1.00, Arctic Data archive System (ADS) [data set], https://doi.org/10.17592/001.2024102244, 2025d.

Harazono, Y. and Takagi, K.: JapanFlux2024 CN-In5 Inner Mongolia no grazing, 1.00, Arctic Data archive System (ADS) [data set], https://doi.org/10.17592/001.2024102245, 2025e.

Harazono, Y. and Takagi, K.: JapanFlux2024 CN-In6 Inner Mongolia heavy grazing, 1.00, Arctic Data archive System (ADS) [data set], https://doi.org/10.17592/001.2024102246, 2025f.

Harazono, Y. and Takagi, K.: JapanFlux2024 CN-In7 Inner Mongolia light grazing, 1.00, Arctic Data archive System (ADS) [data set], https://doi.org/10.17592/001.2024102247, 2025g.

Harazono, Y. and Takagi, K.: JapanFlux2024 CN-In8 Inner Mongolia medium grazing, 1.00, Arctic Data archive System (ADS) [data set], https://doi.org/10.17592/001.2024102248, 2025h.

Harazono, Y., Kim, J., Miyata, A., Choi, T., Yun, J.-I.,and Kim, J.-W.: Measurement of energy budget components during the International Rice Experiment (IREX) in Japan, Hydrol. Process., 12, 2081–2092, https://doi.org/10.1002/(SICI)1099-1085(19981030)12:13/14<2081::AID-HYP721>3.0.CO;2-M, 1998.

Harazono, Y., Takagi, K., and Miyata, A.: JapanFlux2024 JP-KaP Kasumigaura lotus paddy, 1.00, Arctic Data archive System (ADS) [data set], https://doi.org/10.17592/001.2024102238, 2025.

Harazono, Y., Yamada, C., and Nishizawa, T.: Characteristics of Aerodynamic Parameters and Turbulent Transport of Momentum and CO_2 Over a Soybean Canopy, Bull. Environ. Res. Cent., the University of Tsukuba, 16, 13–25, 1992.

Hersbach, H., Bell, B., Berrisford, P., Hirahara, S., Horányi, A., Muñoz-Sabater, J., Nicolas, J., Peubey, C., Radu, R., Schepers, D., Simmons, A., Soci, C., Abdalla, S., Abellan, X., Balsamo, G., Bechtold, P., Biavati, G., Bidlot, J., Bonavita, M., De Chiara, G., Dahlgren, P., Dee, D., Diamantakis, M., Dragani, R., Flemming, J., Forbes, R., Fuentes, M., Geer, A., Haimberger, L., Healy, S., Hogan, R. J., Hólm, E., Janisková, M., Keeley, S., Laloyaux, P., Lopez, P., Lupu, C., Radnoti, G., de Rosnay, P., Rozum, I., Vamborg, F., Villaume, S., and Thépaut, J.-N.: The ERA5 global reanalysis, Q. J. Roy. Meteor. Soc. 146, 1999–2049, https://doi.org/10.1002/qj.3803, 2020.

Hirano, T.: JapanFlux2024 JP-Sb1 Sarobetsu Mire Moss, 1.00, Arctic Data archive System (ADS) [data set], https://doi.org/10.17592/001.2024102216, 2025a.

Hirano, T.: JapanFlux2024 JP-Sb2 Sarobetsu Mire Sasa, 1.00, Arctic Data archive System (ADS) [data set], https://doi.org/10.17592/001.2024102217, 2025b.

Hirano, T. and Hirata, R.: JapanFlux2024 JP-Tmd Tomakomai Flux Research Site Disturbed, 1.00, Arctic Data archive System (ADS) [data set], https://doi.org/10.17592/001.2024102230, 2025.

Hirano, T., Hirata, R., Fujinuma, Y., Saigusa, N., Yamamoto, S., Harazono, Y., Takada, M., Inukai, K., and Inoue, G.: CO_2 and water vapor exchange of a larch forest in northern Japan, Tellus B, 55, 244–257, https://doi.org/10.3402/tellusb.v55i2.16753, 2003.

Hirano, T. and Ohkubo, S.: JapanFlux2024 ID-PaB Palangkaraya Drained Burnt forest, 1.00, Arctic Data archive System (ADS) [data set], https://doi.org/10.17592/001.2024102213, 2025a.

Hirano, T. and Ohkubo, S.: JapanFlux2024 ID-PaD Palangkaraya drained forest, 1.00, Arctic Data archive System (ADS) [data set], https://doi.org/10.17592/001.2024102232, 2025b.

Hirano, T. and Ohkubo, S.: JapanFlux2024 ID-Pag Palangkaraya Undrained Forest, 1.00, Arctic Data archive System (ADS) [data set], https://doi.org/10.17592/001.2024102233, 2025c.

Hirano, T., Yamada, H., Takada, M., Fujimura, Y., Fujita, H., and Takahashi, H.: Effects of the expansion of vascular plants in Sphagnum-dominated bog on evapotranspiration, Agr. Forest Meteorol., 220, 90–100, https://doi.org/10.1016/j.agrformet.2016.01.039, 2016.

Hirano, T., Suzuki, K., and Hirata, R.: Energy balance and evapotranspiration changes in a larch forest caused by severe disturbance during an early secondary succession, Agr. Forest Meteorol., 232, 457–468, https://doi.org/10.1016/j.agrformet.2016.10.003, 2017.

Hirano, T., Ohkubo, S., Itoh, M., Tsuzuki, H., Sakabe, A., Takahashi, H., Kusin, K., and Osaki, M.: Large variation in carbon dioxide emissions from tropical peat swamp forests due to disturbances, Comm. Earth Environ., 5, 221, https://doi.org/10.1038/s43247-024-01387-7, 2024.

Hirata, R. and Hirano, T.: JapanFlux2024 JP-Tmk Tomakomai Flux Research Site, 1.00, Arctic Data archive System (ADS) [data set], https://doi.org/10.17592/001.2024102222, 2025.

Hirata, R., Saigusa, N., Yamamoto, S., Ohtani, Y., Ide, R., Asanuma, J., Gamo, M., Hirano, T., Kondo, H., Kosugi, Y., Li, S. -G., Nakai, Y., Takagi, K., Tani, M., and Wang, H.: Spatial distribution of carbon balance in forest ecosystems across East Asia, Agr. Forest Meteorol., 148, 761–775, https://doi.org/10.1016/j.agrformet.2007.11.016, 2008.

Hiyama, T., Kochi, K., Kobayashi, N., and Sirisampan, S.: Seasonal variation in stomatal conductance and physiological factors observed in a secondary warm-temperate forest, Ecol. Res., 20, 333–346, https://doi.org/10.1007/s11284-005-0049-6, 2005.

Ichii, K., Ueyama, M., Kondo, M., Saigusa, N., Kim, J., Alberto, M. C., Ardö, J., Euskirchen, E., Kang, M., Hirano, T., Joiner, J., Kobayashi, H., Marchesini, L. B., Merbold, L., Miyata, A., Saitoh, T. M., Takagi, K., Varlagin, A., Bret-Harte, M. S., Kitamura, K., Kosugi, Y., Kotani, A., Kumar, K., Li, S. -G., Machimura, T., Matsuura, Y., Mizoguchi, Y., Ohta, T., Mukherjee, S., Yanagi, Y., Yasuda, Y., Zhang, Y., and Zhao, F.: New data-driven estimation of terrestrial CO_2 fluxes in Asia using a standardized database of eddy covariance measurements, remote sensing data, and support vector regression, J. Geophys. Res.-Biogeo., 122, 767–795, https://doi.org/10.1002/2016JG003640, 2017.

Igarashi, Y., Katul, G. G., Kumagai, T., Yoshifuji, N., Sato, T., Tanaka, N., Tanaka, K., Fujinami, H., Suzuki, M., and Tantasirin, C.: Separating physical and biological controls on long-term evapotranspiration fluctuations in a tropical deciduous forest subjected to monsoonal rainfall, J. Geophys. Res.-Biogeo., 120, 1262–1278, https://doi.org/10.1002/2014JG002767, 2015.

Iida, S., Shimizu, T., Shinohara, Y., Takeuchi, S., and Kumagai, T.: The necessity of sensor calibration for the precise measurement of water fluxes in forest ecosystems, in: Forest-Water Interactions, Ecological Studies, edited by: Levia, D. F., Carlyle-Moses, D. E., Iida, S., Michalzik, B., Nanko, K., Tischer, A., vol. 240, Springer, Cham, https://doi.org/10.1007/978-3-030-26086-6_2, 2020.

Ishida, S.: JapanFlux2024 JP-Srk Shirakami Beech Forest Site, 1.00, Arctic Data archive System (ADS) [data set], https://doi.org/10.17592/001.2024102218, 2025.

Ishida S., Ito, D., and Matsuura, Y.: Overview of Shirakami Flux Tower and General Meteorological Conditions between July and October, 2008, Shirakami Kenkyu, 6, 18–25, 2009 (in Japanese with English abstract).

Ishikawa, M.: JapanFlux2024 MN-Udg Udleg practice forest,1.00, Arctic Data archive System (ADS) [data set], https://doi.org/10.17592/001.2024121017, 2025.

Iwahana, G., Machimura, T., Kobayashi, Y., Fedorov, A. N., Konstantinov, P. Y., and Fukuda, M.; Influence of forest clear-cutting on the thermal and hydrological regime of the active layer near Yakutsk, eastern Siberia, J. Geophys. Res., 110, G02004, https://doi.org/10.1029/2005JG000039, 2005.

Iwata, H.: JapanFlux2024 JP-Nkm Nishikoma Site, 1.00, Arctic Data archive System (ADS) [data set], https://doi.org/10.17592/001.2024102231, 2025a.

Iwata, H.: JapanFlux2024 JP-SwL Suwa Lake Site, 1.00, Arctic Data archive System (ADS) [data set], https://doi.org/10.17592/001.2024102219, 2025b.

Iwata, H. and Suzuki, J.: JapanFlux2024 JP-Shn Shinshu University Experimental Forest Site, 1.00, Arctic Data archive System (ADS) [data set], https://doi.org/10.17592/001.2024121009, 2025.

Iwata, H., Hirata, R., Takahashi, Y., Miyabara, Y., Itoh, M., and Iizuka, K.: Partitioning eddy-covariance methane fluxes from a shallow lake into diffusive and ebullitive fluxes, Bound.-Lay. Meteorol., 169, 413–428, https://doi.org/10.1007/s10546-018-0383-1, 2018.

Kabeya, N., Shimizu, A., Shimizu, T., Iida, S., Tamai, K., Miyamato, A., Chann, S., Araki, M., and Ohnuki, Y.: Long-term Hydrological Observations in a Lowland Dry Evergreen Forest Catchment Area of the Lower Mekong River, Cambodia, JARQ-Jpn. Agr. Res. Q., 55, 177–190, https://doi.org/10.6090/jarq.55.177, 2021.

Kanda, M. and Moriwaki, R.: JapanFlux2024 JP-Kgu Kugahara urban residential area, 1.00, Arctic Data archive System (ADS) [data set], https://doi.org/10.17592/001.2024121018, 2025.

Kang, M. and Cho, S.: Progress in water and energy flux studies in Asia: A review focused on eddy covariance measurements, J. Agric. Meteorol., 77, 2–23, https://doi.org/10.2480/agrmet.D-20-00036, 2021.

Kato, T. and Tang, Y.: Spatial variability and major controlling factors of CO_2 sink strength in Asian terrestrial ecosystems: evidence from eddy covariance data, Glob. Change Biol., 14, 2333–2348, https://doi.org/10.1111/j.1365-2486.2008.01646.x, 2008.

Keenan, T. F., Luo, X., Stocker, B. D., De Kauwe, M. G., Medlyn, B. E., Prentice, I. C., Smith, N. G., Terrer, C., Wang, H., Zhang, Y., and Zhou, S.: A constraint on historic growth in global photosynthesis due to rising CO_2, Nat. Clim. Change, 13, 1376–1381, https://doi.org/10.1038/s41558-023-01867-2, 2023.

Kitamura, K., Shimizu, T., Kominami, Y., Hagino, K., Mizoguchi, Y., Tamai, K. Shimizu, A., Ohnuki, Y., Kobayashi, M.: JapanFlux2024 JP-Khw Kahoku Experiment watershed, 1.00, Arctic Data archive System (ADS) [data set], https://doi.org/10.17592/001.2024121005, 2025.

Knox, S. H., Jackson, R. B., Poulter, B., McNicol, G., Fluet-Chouinard, E., Zhang, Z., Hugelius, G., Bousquet, P., Canadell,

J. G., Saunois, M., Papale, D., Chu, H., Keenan, T. F., Baldocchi, D., Torn, M. S., Mammarella, I., Trotta, C., Aurela, M., Bohrer, G., Campbell, D. I., Cescatti, A., Chamberlain, S., Chen, J., Chen, W., Dengel, S., Desai, A. R., Euskirchen, E., Friborg, T., Gasbarra, D., Goded, I., Goeckede, M., Heimann, M., Helbig, M., Hirano, T., Hollinger, D. Y., Iwata, H., Kang, M., Klatt, J., Krauss, K. W., Kutzbach, L., Lohila, A., Mitra, B., Morin, T. H., Nilsson, M. B., Niu, S., Noormets, A., Oechel, W. C., Peichl, M., Peltola, O., Reba, M. L., Richardson, A. D., Runkle, B. R., Ryu, Y., Sachs, T., Schäfer, K. B. R., Schmid, H. P., Shurpali, N., Sonnentag, O., Tang, A. C. I., Ueyama, M., Vargas, R., Vesala, T., Ward, E. J., Windham-Myers, L., Wohlfahrt, G., and Zona, D.: FLUXNET-CH_4 synthesis activity: objectives, observations, and future directions, B. Am. Meteorol. Soc., 100, 2607–2632, https://doi.org/10.1175/BAMS-D-18-0268.1, 2019.

Kominami, Y., Jomura, M., Dannoura, M., Goto, Y., Tamai, K., Miyama, T., Kanazawa, Y., Kaneko, S., Okumura, M., Misawa, N., Hamada, S., Sasaki, T., Kimura, H., and Ohtani, Y.: Biometric and eddy-covariance-based estimates of carbon balance for a warm-temperate mixed forest in Japan, Agr. Forest Meteorol., 148, 723–737, https://doi.org/10.1016/j.agrformet.2008.01.017, 2008.

Komiya, S.: Methane and carbon dioxide dynamics in temperate and tropical rice paddy fields, PhD thesis, Meiji University, 118 pp., https://meiji.repo.nii.ac.jp/records/14850 (last access: 27 December 2024), 2015.

Komiya, S.: JapanFlux2024 JP-Hrt Hiratsuka Rice Paddy, 1.00, Arctic Data archive System (ADS) [data set], https://doi.org/10.17592/001.2024121020, 2025a.

Komiya, S.: JapanFlux2024 TH-Kms Kamphaeng Saen Rice Paddy, 1.00, Arctic Data archive System (ADS) [data set], https://doi.org/10.17592/001.2024121021, 2025b.

Kosugi, Y. and Takanashi, S.: JapanFlux2024 JP-Ako JP-Ako Akou green belt, 1.00, Arctic Data archive System (ADS) [data set], https://doi.org/10.17592/001.2024121001, 2025.

Kosugi, Y., Tanaka, H., Takanashi, S., Matsuo, N., Ohte, N., Shibata, S., and Tani, M.: Three years of carbon and energy fluxes from Japanese evergreen broadleaved forest, Agr. Forest Meteorol., 132, 329–343, https://doi.org/10.1016/j.agrformet.2005.08.010, 2005.

Kotani, A. and Ohta, T.: JapanFlux2024 JP-SMF Seto Mixed Forest Site, 1.00, Arctic Data archive System (ADS) [data set], https://doi.org/10.17592/001.2024102234, 2025.

Kotani, A., Kononov, A. V., Ohta, T., and Maximov, T. C.: Temporal variations in the linkage between the net ecosystem exchange of water vapour and CO_2 over boreal forests in eastern Siberia, Ecohydrology, 7, 209–225, https://doi.org/10.1002/eco.1449, 2014.

Kotani, A., Ohta, T., Yabuki, H., Maximov, T., and Petrov, R.: JapanFlux2024 RU-Sk2 Yakutsk Pine, 1.00, Arctic Data archive System (ADS) [data set], https://doi.org/10.17592/001.2024102236, 2025.

Kumagai, T. and Takamura, N.: JapanFlux2024 TH-Kog Kog-Ma Watershed, 1.00, Arctic Data archive System (ADS) [data set], https://doi.org/10.17592/001.2024121023, 2025a.

Kumagai, T. and Takamura, N.: JapanFlux2024 TH-Mae Mae Moh plantation, 1.00, Arctic Data archive System (ADS) [data set], https://doi.org/10.17592/001.2024121024, 2025b.

Kumagai, T., Hata, Y., Matsumoto, K., and Kume, T.: JapanFlux2024 MY-LHP Lambir Hills National Park, 1.00, Arctic Data archive System (ADS) [data set], https://doi.org/10.17592/001.2024102206, 2025.

Kume, T., Takizawa, H., Yoshifuji, N., Tanaka, K., Tantasirin, C., Tanaka, N., and Suzuki, M.: Impact of soil drought on sap flow and water status of evergreen trees in a tropical monsoon forest in northern Thailand, Forest Ecol. Manag., 238, 220–230, https://doi.org/10.1016/j.foreco.2006.10.019, 2007.

Lasslop, G., Reichstein, M., Papale, D., Richardson, A. D., Arneth, A., Barr, A., Stoy, P., and Wohlfahrt, G.: Separation of net ecosystem exchange into assimilation and respiration using a light response curve approach: critical issues and global evaluation, Glob. Change Biol., 16, 187–208, https://doi.org/10.1111/j.1365-2486.2009.02041.x, 2010.

Li, S. G., Harazono, Y., Oikawa, T., Zhao, H. L., He, Z. Y., and Chang, X. L.: Grassland desertification by grazing and the resulting micrometeorological changes in Inner Mongolia, Agr. Forest Meteorol., 102, 125–137, https://doi.org/10.1016/S0168-1923(00)00101-5, 2000.

Li, S.-G., Asanuma, J., Eugster, W., Kotani, A., Davaa, G., Oyunbaatar, D., and Sugita, M.: Net ecosystem carbon dioxide exchange over grazed steppe in central Mongolia, Glob. Change Biol., 11, 1941–1955, https://https://doi.org/10.1111/j.1365-2486.2005.01047.x, 2005a.

Li, S.-G., Asanuma, J., Kotani, A., Eugster, W., Davaa, G., Oyunbaatar, D., and Sugita, M.: Year-round measurements of net ecosystem CO_2 flux over a montane larch forest in Mongolia, J. Geophys. Res., 110, D0930, https://https://doi.org/10.1029/2004JD005453, 2005b.

Liu, H. Z., Feng, J. W., Järvi, L., and Vesala, T.: Four-year (2006–2009) eddy covariance measurements of CO_2 flux over an urban area in Beijing, Atmos. Chem. Phys., 12, 7881–7892, https://doi.org/10.5194/acp-12-7881-2012, 2012.

Lloyd, J. and Taylor, J. A.: On the temperature dependence of soil respiration, Funct. Ecol., 8, 315323, https://doi.org/10.2307/2389824, 1994.

Machimura, T.: JapanFlux2024 RU-NeB Neleger Burnt Forest, 1.00, Arctic Data archive System (ADS) [data set], https://doi.org/10.17592/001.2024102210, 2025a.

Machimura, T.: JapanFlux2024 RU-NeC Neleger Cutover, 1.00, Arctic Data archive System (ADS) [data set], https://doi.org/10.17592/001.2024102211, 2025b.

Machimura, T.: JapanFlux2024 RU-NeF Neleger larch forest, 1.00, Arctic Data archive System (ADS) [data set], https://doi.org/10.17592/001.2024102212, 2025c.

Matsuda, K., Watanabe, I., Mizukami, K., Ban, S., and Takahashi, A.: Dry deposition of $PM_{2.5}$ sulfate above a hilly forest using relaxed eddy accumulation, Atmos. Environ., 107, 255–261, https://doi.org/10.1016/j.atmosenv.2015.02.050, 2015.

Matsumoto, K., Ohta, T., Nakai, T., Kuwada, T., Daikoku, K., Iida, S., Yabuki, H., Kononov, A. V., van der Molen, M. K., Kodama, Y., Maximov, T. C., Dolman, A. J., and Hattori, S.: Energy consumption and evapotranspiration at several boreal and temperate forests in the Far East, Agr. Forest Meteorol., 148, 1978–1989, https://doi.org/10.1016/j.agrformet.2008.09.008, 2008.

Matsumoto, K., Terasawa, K., Taniguchi, S., Ohashi, M., Katayama, A., Kume, T., and Takashima, A.: Spatial and seasonal variations in soil respiration in a subtropical forest in Okinawa, Japan, Ecol. Res., 38, 367–490, https://doi.org/10.1111/1440-1703.12386, 2023.

Matsumoto, K., Taniguchi, S., and Takashima, A.: JapanFlux2024 JP-Ynf Yona-Field Tower Site, 1.00, Arctic Data archive System (ADS) [data set], https://doi.org/10.17592/001.2024102225, 2025.

Matsuo, T. and Sasyo, Y.: Non-melting phenomena of snowflakes observed in subsaturated air below freezing level, J. Meteorol. Soc. Jpn, 59, 26–32, https://doi.org/10.2151/jmsj1965.59.1_26, 1981.

Matsuura, S.: JapanFlux2024 JP-NsM Nasu Research Station, Manure Application Plot, 1.00, Arctic Data archive System (ADS) [data set], https://doi.org/10.17592/001.2024121028, 2025a.

Matsuura, S.: JapanFlux2024 JP-NsC Nasu Research Station, Manure Application Plot, 1.00, Arctic Data archive System (ADS) [data set], https://doi.org/10.17592/001.2024121029, 2025b.

Matsuura, S., Mori, A., Miyata, A., and Hatano, R.: Effects of farmyard manure application and grassland renovation on net ecosystem carbon balance in a temperate grassland: analysis of 11-year eddy covariance data, J. Agric. Meteorol., 79, 2–17, https://doi.org/10.2480/agrmet.D-22-00007, 2023.

Matsuura, Y. and Morishita, T.: JapanFlux2024 RU-Tur Tura, 1.00, Arctic Data archive System (ADS) [data set], https://doi.org/10.17592/001.2024102223, 2025.

Maximov, T., Kotani, A., Petrov, R., Hiyama, T., and Ohta, T.: JapanFlux2024 RU-Ege Elgeeii forest station, 1.00, Arctic Data archive System (ADS) [data set], https://doi.org/10.17592/001.2024102229, 2025a.

Maximov, T., Kotani, A., Petrov, R., Iijima, Y., Yabuki, H., Hiyama, T., and Ohta, T.: JapanFlux2024 RU-SkP Yakutsk Spasskaya Pad larch, 1.00, Arctic Data archive System (ADS) [data set], https://doi.org/10.17592/001.2024102235, 2025b.

Medlyn, B. E., Duursma, R. A., Eamus, D., Ellsworth, D. S., Prentice, I. C., Barton, C. V., Crous, K. Y., De Angelis, P., Freeman, M, and Wingate, L.: Reconciling the optimal and empirical approaches to modelling stomatal conductance, Glob. Change Biol., 17, 2134–2144, https://doi.org/10.1111/j.1365-2486.2010.02375.x, 2011.

Miyata, A., Harazono, Y., Yoshimoto, M., and Terai, H.: The influence of temperature on CO2 and methane fluxes at a flooded boreal wetland in Hokkaido, Japan, J. Agric. Meteorol., 52, 807–810, https://doi.org/10.2480/agrmet.52.807, 1997.

Miyata, A., Harazono, Y., Kim, J., Terai, H., Takahashi, H., and Nishio, F.: Carbon dioxide and methane fluxes at Kushiro Mire, in: Proc. International Workshop for Advanced Flux Network and Flux Evaluation, Sapporo, Japan, 27–29 September 2000, 29–32, https://cger.nies.go.jp/publications/report/m011/m011_2001.html (last access: 27 December 2024), 2001.

Miyazaki, S., Ishikawa, M., Baatarbileg, N., Damdinsuren, S., Ariuntuya, N., and Jambaljav, Y.: Interannual and seasonal variations in energy and carbon exchanges over the larch forests on the permafrost in northeastern Mongolia, Polar Sci., 8, 166–182, https://doi.org/10.1016/j.polar.2013.12.004, 2014.

Mizoguchi, Y. and Kitamura, K.: JapanFlux2024 JP-Spp Sapporo forest meteorology research site, 1.00, Arctic Data archive System (ADS) [data set], https://doi.org/10.17592/001.2024121010, 2025.

Mizoguchi, Y., Miyata, A., Ohtani, Y., Hirata, R., and Yuta, S.: A review of tower flux observation sites in Asia, J. Forest Res.-Jpn., 14, 1–9, https://doi.org/10.1007/s10310-008-0101-9, 2009.

Mizoguchi, Y., Ohtani, Y., Takanashi, S., Iwata, H., Yasuda, Y., and Nakai, Y.: Seasonal and interannual variation in net ecosystem production of an evergreen needleleaf forest in Japan, J. Forest Res.-Jpn., 17, 283–295, https://doi.org/10.1007/s10310-011-0307-0, 2012.

Moriwaki, R. and Kanda, M.: Seasonal and diurnal fluxes of radiation, heat, water vapor, and carbon dioxide over a suburban area, J. Appl. Meteorol., 43, 1700–1710, https://doi.org/10.1175/JAM2153.1, 2004.

Murayama, S., Kondo, H., Ishidoya, S., Maeda, T., Saigusa, N., Yamamoto, S., Kamezaki, K., and Muraoka, H.: Interannual variation and trend of carbon budget observed for more than two decades at Takayama in a cool-temperate deciduous forest in central Japan, J. Geophys. Res.-Biogeo., 129, e2023JG007769, https://doi.org/10.1029/2023JG007769, 2024a.

Murayama, S., Kondo, H., Muraoka, H., Ishidoya, S., and Maeda, T.: JapanFlux2024 JP-Tak Takayama deciduous broadleaf forest site, 1.00, Arctic Data archive System (ADS) [data set], https://doi.org/10.17592/001.2024102221, 2025b.

Nagano, H. and Hasegawa, H.: JapanFlux2024 JP-Mra Muramatsu agricultural field, 1.00, Arctic Data archive System (ADS) [data set], https://doi.org/10.17592/001.2024102209, 2025.

Nakai, T., van der Molen, M. K., Gash, J. H. C., and Kodama, Y.: Correction of sonic anemometer angle of attack errors, Agr. Forest Meteorol., 136, 19–30, https://doi.org/10.1016/j.agrformet.2006.01.006, 2006.

Nakai, T., Kim, Y., Busey, R. C., Suzuki, R., Nagai, S., Kobayashi, H., Park, H., Sugiura, K., and Ito, A.: Characteristics of evapotranspiration from a permafrost black spruce forest in interior Alaska, Polar Sci., 7, 136–148, https://doi.org/10.1016/j.polar.2013.03.003, 2013.

Nakai, T., Ohta, T., Kodama, Y., Sumida, A., Toda, M., and Hara, T.: JapanFlux2024 JP-MBF Moshiri Birch Forest Site, 1.00, Arctic Data archive System (ADS) [data set], https://doi.org/10.17592/001.2024102207, 2025a.

Nakai, T., Ohta, T., Kodama, Y., Sumida, A., Toda, M., and Hara, T.: JapanFlux2024 JP-MMF Moshiri Mixed Forest Site, 1.00, Arctic Data archive System (ADS) [data set], https://doi.org/10.17592/001.2024102208, 2025b.

Nakai, Y., Matsuura, Y., Kajimoto, T., Abaimov, A. P., Yamamoto, S., and Zyryanova, O. A.: Eddy covariance CO_2 flux above a Gmelin larch forest on continuous permafrost in Central Siberia during a growing season, Theor. Appl. Climatol., 93, 133–147, https://doi.org/10.1007/s00704-007-0337-x, 2008.

Nakaji, T.: JapanFlux2024 JP-Tom Tomakomai Experimental Forest, 1.00, Arctic Data archive System (ADS) [data set], https://doi.org/10.17592/001.2024121015, 2025.

Nakaji, T., Nakamura, M., and Ide, R.: JapanFlux2024 JP-Toc Tomakomai Crane site, 1.00, Arctic Data archive System (ADS) [data set], https://doi.org/10.17592/001.2024121014, 2025.

Nakamura, M., Nakaji, T., Muller, O., and Hiura, T.. Different initial responses of the canopy herbivory rate in mature oak trees to experimental soil and branch warming in a soil-freezing area, OIKOS, 124, 8, 1071–1077, https://doi.org/10.1111/oik.01940, 2014

Nakaya, K., Suzuki, C., Kobayashi, T., Ikeda, H., and Yasuike, S.: Application of a displaced-beam small aperture scintillometer to a deciduous forest under unstable atmospheric conditions, Agr. Forest Meteorol., 136, 45–55, https://doi.org/10.1016/j.agrformet.2005.12.009, 2006.

Nakaya, K., Suzuki, C., Kobayashi, T., Ikeda, H., and Yasuike, S.: JapanFlux2024 JP-Kzw Karuizawa, 1.00, Arctic Data archive System (ADS) [data set], https://doi.org/10.17592/001.2024102205, 2025.

Nie, D., Demetriades-Shah, T., and Kanemasu, E. T.: Surface energy fluxes on four slope sites during FIFE 1988, J. Geophys. Res.-Atmos., 97, 18641–18649, https://doi.org/10.1029/91JD03043, 1992.

Ohta, T., Maximov, T. C., Dolman, A. J., Nakai, T., van der Molen, M. K., Kononov, A. V., Maximov, A. P., Hiyama, T., Iijima, Y., Moors, E. J., Tanaka, H., Toba, T., and Yabuki, H.: Interannual variation of water balance and summer evapotranspiration in an eastern Siberian larch forest over a 7-year period (1998–2006), Agr. Forest Meteorol., 148, 1941–1953, https://doi.org/10.1016/j.agrformet.2008.04.012, 2008.

Ohtaki, E.: Application of an infrared carbon dioxide and humidity instrument to studies of turbulent transport, College of Liberal Art. Sci., 29, 85–107, 1984.

Ohkubo, S., Hirano, T., and Kusin, K.: Assessing the carbon dioxide balance of a degraded tropical peat swamp forest following multiple fire events of different intensities, Agr. Forest Meteorol., 306, 108448, https://doi.org/10.1016/j.agrformet.2021.108448, 2021.

Ono, K.: JapanFlux2024 JP-Mse Mase paddy flux site, 1.00, Arctic Data archive System (ADS) [data set], https://doi.org/10.17592/001.2024121007, 2025.

Papale, D., Reichstein, M., Aubinet, M., Canfora, E., Bernhofer, C., Kutsch, W., Longdoz, B., Rambal, S., Valentini, R., Vesala, T., and Yakir, D.: Towards a standardized processing of Net Ecosystem Exchange measured with eddy covariance technique: algorithms and uncertainty estimation, Biogeosciences, 3, 571–583, https://doi.org/10.5194/bg-3-571-2006, 2006.

Pastorello, G., Trotta, C., Canfora, E., et al.: The FLUXNET2015 dataset and the ONEFlux processing pipeline for eddy covariance data, Sci. Data, 7, 225, https://doi.org/10.1038/s41597-020-0534-3, 2020.

Saigusa, N. and Wang, H.: JapanFlux2024 CN-Lsh Laoshan,1.00, Arctic Data archive System (ADS) [data set], https://doi.org/10.17592/001.2024121006, 2025.

Saigusa, N., Li, S.-G., Kwon, H., Takagi, K., Zhang, L.-M., Ide, R. Ueyama, M., Asanuma, J., Choi, Y.-J., Chun, J. H., Han, S.-J., Hirano, T., Hirata, R., Kang, M., Kato, T., Kim, J., Li, Y.-N., Maeda, T., Miyata, A., Mizoguchi, Y., Murayama, S., Nakai, Y., Ohta, T., Saitoh, T. M., Wang, H.-M., Yu, G.-R., Zhang, Y.-P., and Zhao, F.-H.: Dataset of CarboEastAsia and uncertainties in the CO_2 budget evaluation caused by different data processing, J. Forest Res.-Jpn., 18, 41–48, https://doi.org/10.1007/s10310-012-0378-6, 2013.

Saito, M., Miyata, A., Nagai, H., and Yamada, T.: Seasonal variation of carbon dioxide exchange in rice paddy field in Japan, Agr. Forest Meteorol., 135, 93–109, https://https://doi.org/10.1016/j.agrformet.2005.10.007, 2005.

Saitoh, T. M. and Tamagawa, I.: JapanFlux2024 JP-Ta2 Takayama evergreen coniferous forest site, 1.00, Arctic Data archive System (ADS) [data set], https://doi.org/10.17592/001.2024102220, 2025.

Saitoh, T. M., Tamagawa, I., Muraoka, H., Lee, N.-Y. M., Yashiro, Y., and Koizumi, H.: Carbon dioxide exchange in a cool-temperate evergreen coniferous forest over complex topography in Japan during two years with contrasting climates, J. Plant Res., 123, 473–483, https://doi.org/10.1007/s10265-009-0308-7, 2010.

Sakabe, A. and Itoh, M.: JapanFlux2024 JP-Nap Nunoike Agricultural Pond, 1.00, Arctic Data archive System (ADS) [data set], https://doi.org/10.17592/001.2024121025, 2025.

Shibata, H., Hiura, T., Tanaka, Y., Takagi, K., and Koike, T.: Carbon cycling and budget in a forested basin of southwestern Hokkaido, northern Japan, Ecol. Res., 20, 325–331, https://doi.org/10.1007/s11284-005-0048-7, 2005.

Shimizu, T., Kumagai, T., Kobayashi, M., Tamai, K., Iida, S., Kabeya, N., Ikawa, R., Tateishi, M., Miyazawa, Y., and Shimizu, A.: Estimation of annual forest evapotranspiration from a coniferous plantation watershed in Japan (2): Comparison of eddy covariance, water budget and sap-flow plus interception loss, J. Hydrol., 522, 250–264, https://doi.org/10.1016/j.jhydrol.2014.12.021, 2015.

Shimizu, T., Kabeya, N., Iida, S., Tamai, K., Shimizu, A., Chann, S., and Saing, S.: JapanFlux2024 KH-Kmp Kampong Thom Lowland Dry Evergreen Forest, 1.00, Arctic Data archive System (ADS) [data set], https://doi.org/10.17592/001.2024102203, 2025a.

Shimizu, T., Iida, S., Kabeya, N., and Iwagami, S.: JapanFlux2024 JP-Tkb Tsukuba Experimental Watershed, 1.00, Arctic Data archive System (ADS) [data set], https://doi.org/10.17592/001.2024121022, 2025b.

Shimoda, S., Mo, W., and Oikawa, T.: The effects of characteristics of Asian Monsoon climate on interannual CO_2 exchange in a humid temperate C_3/C_4 co-occurring grassland, SOLA, 1, 169–172, https://doi.org/10.2151/sola.2005-044, 2005.

Sugita, M.: JapanFlux2024 JP-KaL Koshin, Lake Kasumigaura, 1.00, Arctic Data archive System (ADS) [data set], https://doi.org/10.17592/001.2024102230, 2025.

Sugita, M., Ogawa, S., and Kawade, M.: Wind as a main driver of spatial variability of surface energy balance over a shallow 10^2-km^2 scale lake: Lake Kasumigaura, Japan, Water Resour. Res., 56, e2020WR027173, https://doi.org/10.1029/2020WR027173, 2020.

Sulla-Menashe, D., Gray, J. M., Abercrombie, S. P., and Friedl, M. A.: Hierarchical mapping of annual global land cover 2001 to present: The MODIS Collection 6 Land Cover product, Remote Sens. Environ., 222, 183–194, https://doi.org/10.1016/j.rse.2018.12.013, 2019.

Takagi, K. and Matsuda, K.: JapanFlux2024 JP-Fmt Field Museum Tama Hills, 1.00, Arctic Data archive System (ADS) [data set], https://doi.org/10.17592/001.2024121003, 2025.

Takagi, K. and Takahashi, Y.: JapanFlux2024 JP-Tef CC-LaG Teshio Experimental Forest, 1.00, Arctic Data archive System (ADS) [data set], https://doi.org/10.17592/001.2024121016, 2025.

Takagi, K., Miyata, A., Harazono, Y., Ota, N., Komine, M., and Yoshimoto, M.: An alternative approach to determining zero-plane displacement,and its application to a lotus paddy field, Agr. Forest Meteorol., 115, 173–181, https://doi.org/10.1016/S0168-1923(02)00209-5, 2003.

Takagi, K., Fukuzawa, K., Liang, N., Kayama, M., Nomura, M., Hojo, H., Sugata, S., Shibata, H., Fukuzawa, T., Takahashi, Y., Nakaji, T., Oguma, H., Mano, M., Akibayashi, Y., Murayama, T., Koike, T., Sasa, K., and Fujinuma, Y.: Change in CO_2 balance under a series of forestry activities in a cool-temperate mixed forest with dense undergrowth, Glob. Change Biol., 15, 1275–1288, https://doi.org/10.1111/j.1365-2486.2008.01795.x, 2009.

Takahashi, Y., Saigusa, N., Hirata, R., ide, R., Fujinuma, Y., Okano, T., and Arase, T.: Characteristics of temporal variations in ecosystem CO_2 exchange in a temperate deciduous needle-leaf forest in the foothills of a high mountain, J. Agric. Meteorol., 71, 302–317, https://doi.org/10.2480/agrmet.D-14-00009, 2015.

Takahashi, Y., Liang, N., Ide, R., Hatsumi, K., Yamao, Y., and Hirose, Y.: JapanFlux2024 JP-Fhk Fuji Hokuroku Flux Observation Site, 1.00, Arctic Data archive System (ADS) [data set], https://doi.org/10.17592/001.2024121002, 2025.

Takamura, N., Hata, Y., Matsumoto, K., Kume, T., Ueyama, M., and Kumagai, T.: El Niño-Southern Oscillation forcing on carbon and water cycling in a Bornean tropical rainforest, P. Natl. Acad. Sci. USA, 120, e2301596120, https://doi.org/10.1073/pnas.2301596120, 2023.

Takanashi, S., Kominami, Y., and Miyama, T.: JapanFlux2024 JP-Fjy Fujiyoshida forest meteorology research site, 1.00, Arctic Data archive System (ADS) [data set], https://doi.org/10.17592/001.2024102202, 2025a.

Takanashi, S., Kominami, Y., and Miyama, T.: JapanFlux2024 JP-Yms Yamashiro forest meteorology research site, 1.00, Arctic Data archive System (ADS) [data set], https://doi.org/10.17592/001.2024102224, 2025b.

Takano, T. and Ueyama, M.: Spatial variations in daytime methane and carbon dioxide emissions in two urban landscapes, Sakai, Japan. Urb. Clim., 36, 100798, https://doi.org/10.1016/j.uclim.2021.100798, 2021.

Takimoto, T. and Iwata, T.: JapanFlux2024 JP-Hc2 Hachihama Experimental Farm, 1.00, Arctic Data archive System (ADS) [data set], https://doi.org/10.17592/001.2024102249, 2025a.

Takimoto, T. and Iwata, T.: JapanFlux2024 JP-Hc3 Hachihama Experimental Farm: Double Crop, 1.00, Arctic Data archive System (ADS) [data set], https://doi.org/10.17592/001.2024102228, 2025b.

Takimoto, T., Iwata, T., Yamamoto, S., and Miura, T.: Characteristics of CO_2 and CH_4 flux at barley-rice double cropping field in southern part of Okayama, J. Agric. Meteorol., 66, 181–191, https://doi.org/10.2480/agrmet.66.3.5, 2010.

Twine, T. E., Kustas, W. P., Norman, J. M., Cook, D. R., Houser, P. R., Meyers, T. P., Prueger, J. H., Starks, P. J., and Wesely, M. L.: Correcting eddy-covariance flux underestimates over a grassland, Agr. Forest Meteorol., 103, 279–300, https://doi.org/10.1016/S0168-1923(00)00123-4, 2000.

Ueyama, M.: JapanFlux2024 JP-Ozm Oizumi Urban Park, 1.00, Arctic Data archive System (ADS) [data set], https://doi.org/10.17592/001.2024072201, 2025a.

Ueyama, M.: JapanFlux2024 JP-Om1 B11 building in Osaka Metropolitan University, 1.00, Arctic Data archive System (ADS) [data set], https://doi.org/10.17592/001.2024072203, 2025b.

Ueyama, M.: JapanFlux2024 JP-Om2 Farm field in Osaka Metropolitan University, 1.00, Arctic Data archive System (ADS) [data set], https://doi.org/10.17592/001.2024072204, 2025c.

Ueyama, M.: JapanFlux2024 JP-Sac Sakai City Office, 1.00, Arctic Data archive System (ADS) [data set], https://doi.org/10.17592/001.2024102215, 2025d.

Ueyama, M. and Ando, T.: Diurnal, weekly, seasonal, and spatial variabilities in carbon dioxide flux in different urban landscapes in Sakai, Japan, Atmos. Chem. Phys., 16, 14727–14740, https://doi.org/10.5194/acp-16-14727-2016, 2016.

Ueyama, M. and Takano, T.: A decade of CO_2 flux measured by the eddy covariance method including the COVID-19 pandemic period in an urban center in Sakai, Japan, Environ. Pollut., 304, 119210, https://doi.org/10.1016/j.envpol.2022.119210, 2022.

Ueyama, M., Ichii, K., Kobayashi, H., Kumagai, T., Beringer, J., Merbold, L., Euskirchen, E., Hirano, T., Belelli M. L., Baldocchi, D., Saitoh, T., Mizoguchi, Y., Ono, K., Kim, J., Varlagin, A., Kang, M., Shimizu, T., Kosugi, Y., Bret-Harte, M., Machimura, T., Matsuura, Y., Ohta, T., Takagi, K., Takanashi, S., and Yasuda, Y.: Inferring CO_2 fertilization effect based on global monitoring land-atmosphere exchange with a theoretical model, Environ. Res. Lett., 15, 084009, https://doi.org/10.1088/1748-9326/ab79e5, 2020a.

Ueyama, M., Yamamori, T., Iwata, H., and Harazono, Y.: Cooling and moistening of the planetary boundary layer in interior Alaska due to a postfire change in surface energy exchange, J. Geophys. Res.-Atmos., 125, e2020JD032968, https://doi.org/10.1029/2020JD032968, 2020b.

Ueyama, M., Yazaki, T., Hirano, T., Futakuchi, and Okamura, M.: Environmental controls on methane fluxes in a cool temperate bog, Agr. Forest Meteorol., 281, 107852, https://doi.org/10.1016/j.agrformet.2019.107852, 2020c.

Ueyama, M., Taguchi, A., and Takano, T.: Water vapor emissions from urban landscapes in Sakai, Japan, J. Hydrol., 598, 126384, https://doi.org/10.1016/j.jhydrol.2021.126384, 2021.

Ueyama, M., Knox, S. H., Delwiche, K. B., Bansal, S., Riley, W. J., Baldocchi, D., Hirano, T., McNicol, G., Schafer, K., Windham-Myers, L., Poulter, B., Jackson, R. B., Chang, K.-Y., Chen, J., Chu, H., Desai, A. R., Gogo, S., Iwata, H., Kang, M., Mammarella, I., Peichl, M., Sonnentag, O., Tuittila, E.-S., Ryu, Y., Euskirchen, E. S., Göckede, M., Jacotot, A., Nilsson, M. B., and Sachs, T.: Modeled production, oxidation, and transport processes of wetland methane emissions in temperate, boreal, and Arctic regions, Glob. Change Biol., 29, 2313–2334, https://doi.org/10.1111/gcb.16594, 2023.

Ueyama, M., Iwata, H., Nagano, H., Kukuu, N., and Harazono, Y.: Anomalous wet summers and rising atmospheric CO_2 concentrations increase the CO_2 sink in a poorly drained forest on permafrost, P. Natl. Acad. Sci. USA, 121, e2414539121 https://doi.org/10.1073/pnas.2414539121, 2024.

Ueyama, M., Hirano, T., and Kominami, Y.: JapanFlux2024 JP-BBY Bibai bog, 1.00, Arctic Data archive System (ADS) [data set], https://doi.org/10.17592/001.2024072202, 2025. TS6

Verma, M., Friedl, M. A., Richardson, A. D., Kiely, G., Cescatti, A., Law, B. E., Wohlfahrt, G., Gielen, B., Roupsard, O., Moors, E. J., Toscano, P., Vaccari, F. P., Gianelle, D., Bohrer, G., Varlagin, A., Buchmann, N., van Gorsel, E., Montagnani, L., and Propastin, P.: Remote sensing of annual terrestrial gross primary productivity from MODIS: an assessment using the

FLUXNET La Thuile data set, Biogeosciences, 11, 2185–2200, https://doi.org/10.5194/bg-11-2185-2014, 2014.

Virkkala, A.-M., Natali, S. M., Rogers, B. M., Watts, J. D., Savage, K., Connon, S. J., Mauritz, M., Schuur, E. A. G., Peter, D., Minions, C., Nojeim, J., Commane, R., Emmerton, C. A., Goeckede, M., Helbig, M., Holl, D., Iwata, H., Kobayashi, H., Kolari, P., López-Blanco, E., Marushchak, M. E., Mastepanov, M., Merbold, L., Parmentier, F.-J. W., Peichl, M., Sachs, T., Sonnentag, O., Ueyama, M., Voigt, C., Aurela, M., Boike, J., Celis, G., Chae, N., Christensen, T. R., Bret-Harte, M. S., Dengel, S., Dolman, H., Edgar, C. W., Elberling, B., Euskirchen, E., Grelle, A., Hatakka, J., Humphreys, E., Järveoja, J., Kotani, A., Kutzbach, L., Laurila, T., Lohila, A., Mammarella, I., Matsuura, Y., Meyer, G., Nilsson, M. B., Oberbauer, S. F., Park, S.-J., Petrov, R., Prokushkin, A. S., Schulze, C., St. Louis, V. L., Tuittila, E.-S., Tuovinen, J.-P., Quinton, W., Varlagin, A., Zona, D., and Zyryanov, V. I.: The ABCflux database: Arctic–boreal CO_2 flux observations and ancillary information aggregated to monthly time steps across terrestrial ecosystems, Earth Syst. Sci. Data, 14, 179–208, https://doi.org/10.5194/essd-14-179-2022, 2022.

Vuichard, N. and Papale, D.: Filling the gaps in meteorological continuous data measured at FLUXNET sites with ERA-Interim reanalysis, Earth Syst. Sci. Data, 7, 157–171, https://doi.org/10.5194/essd-7-157-2015, 2015.

Wang, H., Zu, Y., Saigusa, N., Yamamoto, S., Kondo, H., Yang, F., and Wang, W.: CO_2, water vapor and energy fluxes in a larch forest in northeast China, J. Agric. Meteorol., 60, 549–552, https://doi.org/10.2480/agrmet.549, 2005.

Wang, H., Sun, F., Wang, T., and Liu, W.: Estimation of daily and monthly diffuse radiation from measurements of global solar radiation a case study across China, Renew. Energ., 126, 226–241, https://doi.org/10.1016/j.renene.2018.03.029, 2018.

Wang, Q., Peng, X., Watanabe, M., Batkhishig, O., Okadera, T., and Saito, Y.: Carbon budget in permafrost and non-permafrost regions and its controlling factors in the grassland ecosystems of Mongolia, Glob. Ecol. Conserv., 41, e02373, https://doi.org/10.1016/j.gecco.2023.e02373, 2023.

Wang, Q., Peng, X., Okadera, T., Watanabe, M., Saito, Y., and Batkhishig, O.: JapanFlux2024 MN-Nkh Nalaikh grassland, 1.00, Arctic Data archive System (ADS) [data set], https://doi.org/10.17592/001.2024102227, 2025a.

Wang, Q., Peng, X., Okadera, T., Watanabe, M., Saito, Y., and Batkhishig, O.: JapanFlux2024 MN-Hst Hustai grassland, 1.00, Arctic Data archive System (ADS) [data set], https://doi.org/10.17592/001.2024102226, 2025b.

Wutzler, T., Lucas-Moffat, A., Migliavacca, M., Knauer, J., Sickel, K., Šigut, L., Menzer, O., and Reichstein, M.: Basic and extensible post-processing of eddy covariance flux data with REddyProc, Biogeosciences, 15, 5015–5030, https://doi.org/10.5194/bg-15-5015-2018, 2018.

Yabuki, H., Ishii, Y., and Ohata, T.: Comparison of water and heat balance on grassland and forest in Central Yakutia, East Siberia, in: Proceedings 6th international study Conference on GEWEX in Asia and GAME (GAME CD-ROM Publ. 11), T1HY30Jul04115511, http://www.hyarc.nagoya-u.ac.jp/game/6thconf/html/ (last access: 27 December 2024), 2004.

Yabuki, H., Ishii, Y., and Ohata, T.: JapanFlux2024 RU-Usk Ulakhan Sykkhan Alas, 1.00, Arctic Data archive System (ADS) [data set], https://doi.org/10.17592/001.2024121027, 2025.

Yamanoi, K., Mizoguchi, Y., and Utsugi, H.: Effects of a windthrow disturbance on the carbon balance of a broadleaf deciduous forest in Hokkaido, Japan, Biogeosciences, 12, 6837–6851, https://doi.org/10.5194/bg-12-6837-2015, 2015.

Yasuda, Y.: JapanFlux2024 JP-Api Appi forest meteorology research site, 1.00, Arctic Data archive System (ADS) [data set], https://doi.org/10.17592/001.2024102201, 2025a.

Yasuda, Y.: JapanFlux2024 JP-Kwg Kawagoe forest meteorology research site, 1.00, Arctic Data archive System (ADS) [data set], https://doi.org/10.17592/001.2024102204, 2025b.

Yasuda, Y., Watanabe, T., Ohtani, Y., Okano, M., and Nakayama, K.: Seasonal variation of CO_2 flux over a broadleaf deciduous forest, J. Japan Soc. Hydrol. & Water Resour., 11, 575–585, https://doi.org/10.3178/jjshwr.11.575, 1998.

Yasuda, Y., Saito, T., Hoshino, D., Ono, K., Ohtani, Y., Mizoguchi, Y., and Morisawa, T.: Carbon balance in a cool–temperate deciduous forest in northern Japan: seasonal and interannual variations, and environmental controls of its annual balance, J. Forest Res.-Jpn., 17, 253–267, https://doi.org/10.1007/s10310-011-0298-x, 2012.

Yu, G.-R., Zhu, X.-J., Fu, Y.-L., He, H.-L., Wang, Q.-F., Wen, X.-F., Li, X.-R., Zhang, L.-M., Zhang, L., Su, W., Li, S.-G., Sun, X.-M., Zhang, Y.-P., Zhang, J.-H., Yan, J.-H., Wang, H.-M., Zhou, G.-S., Jia, B.-R., Xiang, W.-H., Li, Y.-N., Zhao, L., Wang, Y.-F., Shi, P.-L., Chen, S.-P., Xin, X.-P., Zhao, F.-H., Wang, Y.-Y., and Tong, C.-L.: Spatial patterns and climate drivers of carbon fluxes in terrestrial ecosystems of China, Glob. Change Biol., 19, 798–810, https://doi.org/10.1111/gcb.12079, 2013.

Zhang, Y., Peña-Arancibia1, J. L., McVicar, T. R., Chiew, F. H. S., Vaze1, J., Liu, C., Lu, X., Zheng, H., Wang, Y., Liu, Y. Y., Miralles, D. G., and Pan, M.: Multi-decadal trends in global terrestrial evapotranspiration and its components, Sci. Rep., 6, 19124, https://https://doi.org/10.1038/srep19124, 2016.

Remarks from the typesetter

TS1 Please note that according to *Earth System Science Data (ESSD)* journal standards, the main DOI(s) and corresponding citation have to appear in the abstract as well (see https://www.earth-system-science-data.net/policies/data_policy.html and https://www.earth-system-science-data.net/submission.html, “Manuscript composition”). I kindly ask you to add the DOI(s) and citation(s). Thank you.

TS2 Please note that the corrections of numbers are not language changes. If you still insist on changing the values in Table 1, the editor has to approve these changes. Please provide an explanation of why these instances need to be changed. We will then ask the editor for approval. Thank you.

TS3 Please note that the year 2022 has to stay since there is no 2022b in the reference list. I apologise for the misunderstanding.

TS4 Please provide direct links to the data sets and DOIs instead of URLs. In any case, please provide a reference list entry including creators, title, and date of last access.

TS5 Please note that this section is mandatory if manuscript was funded. Thank you.

TS6 Please note that the year 2025 has to stay since there are not years 2025a–2025d in the reference list.